

Stony Brook University



OFFICIAL COPY

The official electronic file of this thesis or dissertation is maintained by the University Libraries on behalf of The Graduate School at Stony Brook University.

© All Rights Reserved by Author.

Synthesis of a Novel Sandwich Base Nucleic Acid Analog

A Thesis Presented

by

Xiao Liu

to

The Graduate School

in Partial Fulfillment of the

Requirements

for the Degree of

Master of Science

in

Chemistry

Stony Brook University

August 2013

Stony Brook University

The Graduate School

Xiao Liu

We, the thesis committee for the above candidate for the
Master of Science degree, hereby recommend
acceptance of this thesis.

Dale G. Drueckhammer – Thesis Advisor
Professor, Department of Chemistry

Jonathan G. Rudick – Chair
Assistant Professor, Department of Chemistry

Kathlyn A. Parker – Third Member
Professor, Department of Chemistry

This thesis is accepted by the Graduate School

Charles Taber
Interim Dean of the Graduate School

Abstract of the Thesis

Synthesis of a Novel Sandwich Base Nucleic Acid Analog

by

Xiao Liu

Master of Science

in

Chemistry

Stony Brook University

2013

Nucleic acid mimics and analogs are artificially designed molecular strands that can bind to natural nucleic acids. They have far-reaching diagnostics and therapeutics applications. An ideal nucleic acid mimic should exhibit strong binding affinity to complementary DNA or RNA and excellent resistance to nucleases. Numerous nucleic acid mimics such as PNA, LNA and morpholino oligonucleotides have been studied for decades. In our study, we aim to synthesize novel improved nucleic acid analogs. We have designed various nucleic acid mimics by computational methods. An analog was chosen for synthesis consisting of a piperidine backbone and a “sandwich” base that intercalates adjacent base pairs. This thesis describes the development of synthetic routes to the “sandwich” base and exploration of a route to the piperidine backbone.

Table of Contents

List of Figures.....	v
List of Schemes.....	vi
List of Abbreviations	vii
Chapter 1 Nucleic Acid Analogs and Their Applications	1
Chapter 2 Design and Synthetic Efforts Toward a Novel Nucleic Acid Analog	9
2.1 Designed Novel Nucleic Acid Analogs by Our Group	9
2.2 Synthetic Background.....	13
2.3 Synthesis of the Carboxylic Acid Form of “Sandwich” Base	18
2.4 Synthesis of the Amine Form of “Sandwich” Base	23
2.5 Synthesis of the Piperidine Backbone.....	29
2.6 Conclusion and Future Work.....	34
Chapter 3 Procedures	35
References.....	42
Appendix.....	45

List of Figures

Figure 1. Examples of modified oligonucleotides ⁴	1
Figure 2. Antigene and Antisense inhibition ⁴	2
Figure 3. Chemical structure of PNA ¹¹	3
Figure 4. Chemical structure of LNA monomer	6
Figure 5. Rnase H can be activated by an LNA-DNA hybrid ¹⁷	7
Figure 6. Chemical structure of a morpholino oligonucleotide ²⁷	8
Figure 7. Monomer structures of four furan based backbone	9
Figure 8. Natural and elongated nucleic acid structures	10
Figure 9. Model of our nucleic acid analog bind with elongated nucleic acid.....	10
Figure 10. 3-D figure of the “sandwich” base nucleic acid complex.....	11
Figure 11. Repeating unit structures of “sandwich” base nucleic acid designs	12
Figure 12. Designed structures of “sandwich” base nucleic acids	13
Figure 13. Structure of “sandwich” base nucleic acid with four stereocenters.....	13
Figure 14. Structures of the amine form and carboxylic acid form of the sandwich base	18
Figure 15. TLC plate of methylation of 9,10-phenanthrenequinone.....	20
Figure 16. TLC plates of formylation of 9,10-dimethoxyphenanthrene	21
Figure 17. TLC plate of the oxidation reaction of 9,10-dimethoxyphenanthrene aldehydes.....	22
Figure 18. TLC plate of azidonation of 9,10-dimethoxyphenanthrene aldehydes	28
Figure 19. TLC plates of hydrolysis of carbamoyl azides	28
Figure 20. TLC plate of bromination of t-butyl crotonate	31
Figure 21. TLC plates of alkylation reactions.....	32

List of Schemes

Scheme 1. Michael addition reaction between (R)-N-benzyl-1-phenylethylamine and methyl crotonate gives great stereoselectivity and good yield.....	14
Scheme 2. Tandem Michael addition of the lithium amide to a diendioate ester with complete selectivity	14
Scheme 3. A product with five stereocenters can be formed through tandem Michael addition	14
Scheme 4. Synthesis of piperidine backbone.....	15
Scheme 5. Synthesis of the amine form of "sandwich" base nucleic acid.....	16
Scheme 6. Synthesis of the carboxylic acid form of "sandwich" base nucleic acid.....	17
Scheme 7. Synthesis of the carboxylic acid form of "sandwich" base.....	18
Scheme 8. Synthesis of 9,10-dimethoxyphenanthrene	19
Scheme 9. Formylation of 9,10-dimethoxyphenanthrene.....	20
Scheme 10. Oxidation of mixture of dimethoxyphenanthrene aldehydes	22
Scheme 11. Attempted oxidative nitration of 9,10-dimethoxyphenanthrene	23
Scheme 12. Diazotization of 9,10-dimethoxyphenanthrene	24
Scheme 13. Diazotization of 2,4-dinitroaniline	25
Scheme 14. Synthesis of the amine form of "sandwich" base starting from dimethoxyphenanthrene aldehydes.....	27
Scheme 15. Synthetic route of the substrate diester	29
Scheme 16. Trials for synthesis of t-butyl crotonate	29
Scheme 17. DCC coupling reaction for synthesis of t-butyl crotonate	30
Scheme 18. Synthesis of t-butyl- γ -bromo crotonate.....	30
Scheme 19. Alkylation of t-butyl- γ -bromo crotonate.....	31
Scheme 20. Tandem Michael Addition of the substrate of diester	32
Scheme 21. Bromination follows tandem Michael Addition of the substrate diester	33
Scheme 22. Proposed selective hydrolysis of the piperidine backbone	34

List of Abbreviations

DNA	Deoxyribonucleic Acid
RNA	Ribonucleic Acid
PNA	Peptide Nucleic Acid
LNA	Locked Nucleic Acid
PCR	Polymerase Chain Reaction
TFOs	Triplex-forming Oligonucleotides
RNase H	Ribonuclease H
HIV-1	Human Immunodeficiency Virus -1
SNPs	Single-nucleotide Polymorphisms
MOs	Morpholino Oligonucleotides
GNA	Glycol Nucleic Acid
TNA	Threose Nucleic Acid
UNA	Unlocked Nucleic Acid
SBNA	Sandwich Base Nucleic Acid
MD	Molecular Dynamics
MM/GBSA	Molecular Mechanics/Generalized Born Surface Area
THF	Tetrahydrofuran
TLC	Thin Layer Chromatography
H-NMR	Proton Nuclear Magnetic Resonance spectroscopy
DCC	Dicyclohexylcarbodiimide
DMAP	4-Dimethylaminopyridine
NBS	<i>N</i> -Bromosuccinimide

Chapter 1 Nucleic Acid Analogs and Their Applications

In recent years, nucleic acid derivatives have attracted significant interest for the potential treatment of many diseases and for potential diagnostic applications.¹ Since 1978, many researchers explored the potential of oligonucleotides as potent tools to manipulate gene expression.² Although natural oligonucleotides can specifically bind to their complementary strands, they are very sensitive to nucleases *in vivo*. In order to overcome this weakness, efforts continue to be made for the design of novel oligonucleotides analogs. The ideal analog should have high binding affinity and selectivity, excellent resistance to nucleases and other cellular enzymes, high stability, and an efficient ability to cross biological membranes *in vivo*.¹ Nucleic acid mimics and analogs may differ from the natural counterparts in the pucker-shaped pentose sugar, the nucleobase, or the phosphate backbone moieties (**Figure 1**). These analogs show a broad range of promising applications for the development of gene agents for therapies, genetic analysis, diagnostic devices, and as molecular tools for nucleic acid operations.³ They have also become general and wide used structures for DNA and RNA recognition.

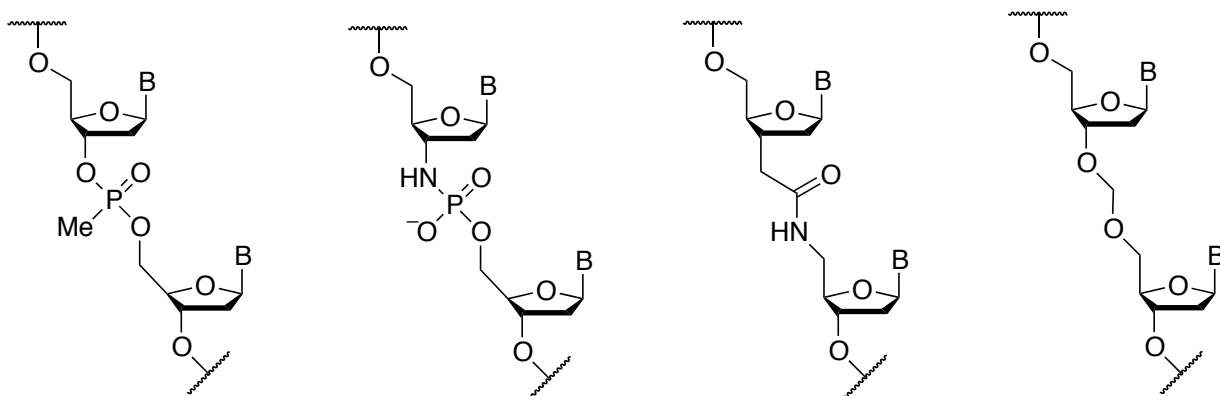


Figure 1. Examples of modified oligonucleotides⁴

Reagents that can specifically bind to double-strand DNA or a single strand DNA or RNA have been researched for decades.⁵ The strategy of antigene and antisense opens up the door for treatment of diseases at the level of gene expression in biochemistry and medicinal chemistry. An antigene oligonucleotide can hybridize double-stranded DNA in the nucleus in order to inhibit the process of transcription (**Figure 2(b)**). Triple helix formation or strand displacement may occur upon binding.⁴ In antisense technology, a short oligonucleotide binds to the mutated gene on mRNA to inhibit the translation process, and therefore the synthesis of a particular protein is terminated (**Figure 2(c)**).⁶ However, a lot of challenges still exist in antigene and antisense strategies. For efficient manipulation of gene expression, a search for effective synthetic oligonucleotide analogues is necessary. Throughout the years, various encouraging nucleic acid analogs and mimics bearing the advantageous properties have been reported, including the peptide nucleic acids (PNAs), locked nucleic acids (LNAs) and morpholino oligonucleotides.

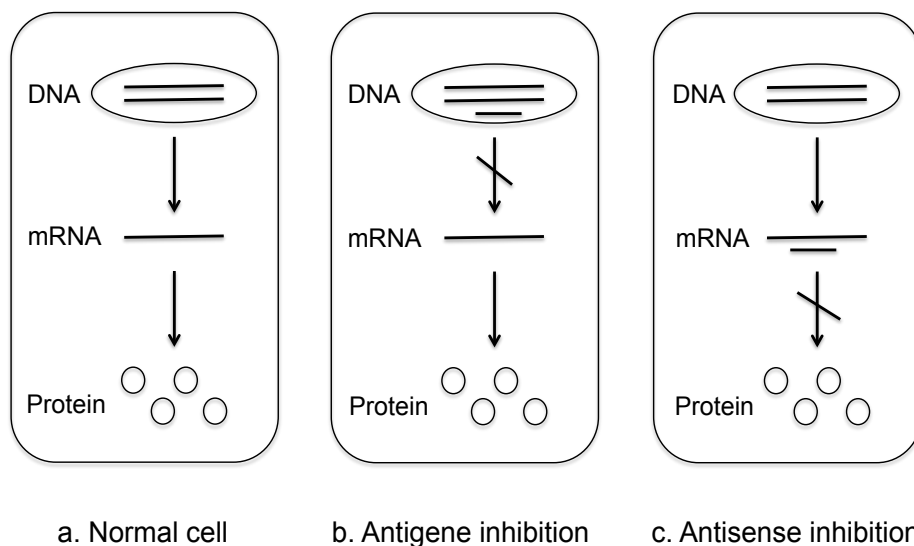


Figure 2. Antigene and Antisense inhibition⁴

Peptide Nucleic Acids were first described by biochemist Peter Nielsen in 1991 in organic chemist Prof. Ole Buchard's laboratory in Copenhagen.⁷ PNA is a DNA mimic and as a lead nucleic acid analogue has exhibited significant promise for developing drugs of gene therapy. PNA shows a major deviation from the natural DNA structure since the total deoxyribose phosphate backbone has been replaced with a synthetic pseudo-peptide backbone generally designed from N-(2-aminoethyl)glycine units, with the nucleobases attached to the backbone nitrogen through the methylenecarbonyl linker (**Figure 3**). The achiral, charge-neutral and relatively flexible polyamide backbone of PNA molecule offers several benefits. Firstly, uncharged PNA oligomers can avoid the electrostatic repulsion with the negatively charged DNA and RNA.⁸ Secondly, this special backbone increases both the affinity and specificity when binding with the complementary DNA and RNA sequences.⁹ Thirdly, compared to the natural antisense oligonucleotides, PNA oligomers exhibit high biostability as they are highly resistant to degradation by nucleases and proteases.¹⁰ Finally, the achiral structure avoids problems of enantiomeric purity.⁴ These features indicate that PNA oligomers are more useful for developing the antisense and antigene product than the natural oligonucleotides. However, the original PNA has some shortcomings such as poor solubility in aqueous media and poor cellular uptake.⁴ Various modifications of PNA have been increasingly developed to address these problems.

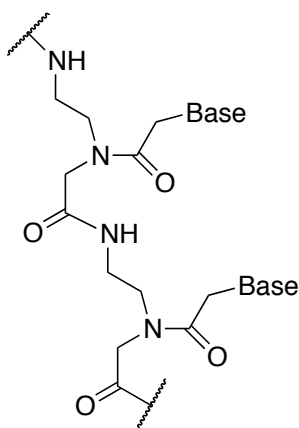


Figure 3. Chemical structure of PNA¹¹

Different PNA/DNA complexes have been designed, including the PNA-DNA/RNA duplexes, PNA-DNA-PNA triplexes and pure PNA-PNA duplexes, etc.⁴ Based on Watson-Crick hydrogen bonding rules, PNAs containing mixed purine/pyridine nucleobases bind to complementary oligonucleotide targets forming duplexes like PNA-DNA, and PNA-RNA. Homopyrimidine PNA oligomers or PNAs, with a high ratio between pyrimidine and purine, bind to complementary oligonucleotides targets forming PNA-DNA-PNA triplexes via Watson-Crick and Hoogsteen hydrogen bonding rules. Investigations show that the identical sequence hybrid thermal stabilities (T_m) follow the order: PNA-PNA > PNA-RNA > PNA-DNA > RNA-DNA > DNA-DNA. Again, because of the uncharged backbone of PNA, the stabilities of PNA hybrids are independent of ionic strength in contrast to the hybrids between two negatively charged oligomers like DNA-DNA or RNA-DNA. The PNA-DNA-PNA triplexes also confer a tighter binding with extremely high thermal stabilities. PNA complexes can be formed in two configurations, and the antiparallel complexes are more stable than the parallel ones. These complexes make PNA a versatile tool for numerous therapeutic and diagnostic applications at the level of gene expression.

PNA has many advantageous properties that make it a potential tool in medical chemistry, molecular biology, genetic diagnostics, and related fields. PNAs have substantial effects on transcription, translation and replication processes *in vitro*.³ PNAs can interfere with the transcription process by their ability to form complexes with DNA. A stable PNA-DNA complex can be formed by PNA targeted against the promoter region that restricts the DNA access of the relevant polymerase. PNA strand displacement complexes, located far downstream from the promoter, also inhibit transcription by resulting in incomplete RNAs. Other research has discovered wide applications of PNAs. An 8-mer PNA (T_8) can efficiently block phage T_3

polymerase activity, as shown by Nielsen et al.¹² Human telomerase activity, which has been found in many categories of human tumors can be inhibited by PNA-RNA complexes in order to arrest the elongation of telomeres *in vitro* experiments.¹³ In diagnostics, specific sequence nucleic acids can be detected and isolated by PNA. The PNA-DNA complexes with high sequence specificity and stability have been adopted into the detection of single base pair mutations in DNA by PCR.¹⁴ PNAs can also cut rare genome when combined with restriction endonucleases.¹⁵

In order to increase the binding affinity towards RNA, many conformational restricted oligonucleotide analogs have been designed in recent years. Locked nucleic acids (LNAs), first described in the Wengel laboratories by Singh et al. in 1998,¹⁶ have been generally studied as RNA mimics. LNA is a bicyclic nucleic acid containing a ribose sugar ring that is locked by a oxymethylene unit between the 2'-carbon and the 4'-carbon atoms as shown in **Figure 4**. This linkage results in a locked 3'-*endo* conformation of the furanose ring in the LNA monomer. Compare to the natural nucleic acids, the close structure allows LNA to better mimic the conformation of the ribose ring in RNA. LNA oligonucleotides can be synthesized using the standard phosphoramidite reagents and synthesizers.¹⁷ Furthermore, LNAs are highly soluble in water like DNA and RNA and can be easy handled. LNAs can be delivered into cells using standard protocols that apply cationic agents due to its charged phosphate backbone.¹⁷ LNAs also have the following features in common with other modified oligonucleotides: (1) high binding affinity to complementary nucleic acids, (2) high bio-stability (resistance to enzymatic degradation), (3) great efficiency as antisense agents *in vivo* and *in vitro*, (4) low toxicity in animals.

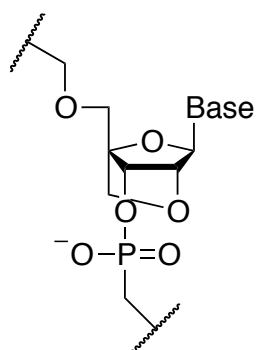


Figure 4. Chemical structure of LNA monomer

As a general tool, LNA has been applied to the process of recognition of ssDNA and ssRNA. The high-affinity LNA can be prepared as fully modified oligomers and mix-mers (LNA-DNA chimera or LNA-RNA chimera). In addition, it is essential to design LNAs or LNA chimera without extensive self-complementary segments because LNAs bind very strongly to a complementary strand. LNAs can also form a triple oligonucleotide by targeting a double-strand DNA (dsDNA). Because of the rigidity of LNAs, fully modified LNA triplex-forming oligonucleotides (TFOs) cannot bind to dsDNA,¹⁸ LNA-DNA chimera with alternating LNA monomers and DNA monomers form the best LNA TFOs.

LNA oligonucleotides have been used widely in the field of gene-silencing technologies and therapeutics and diagnostics. RNase H is one enzyme in human, animal, and bacterial cells that cleaves the RNA strand of DNA-RNA hybrids formed during lagging strand synthesis. RNase H can be activated when DNA oligonucleotides bind to mRNA, leading to the degradation of mRNA.¹⁹ Wahlestedt et al. have observed that LNA-DNA chimeras can readily activate RNase H (**Figure 5**) to cleave the RNA strand.²⁰ Recently, Jakobsen et al. have reported that LNA antisense oligonucleotides are applicable inhibitors of HIV-1 expression.²¹ Like PNA, LNA can also inhibit human telomerase.²² Incorporating LNA monomers into the binding arms of

DNAzymes (Deoxyribozymes) can obtain LNAzymes which display intensely increased efficiency of RNA cleavage.²³ In diagnostics, LNAs have been applied for efficient scanning of single-nucleotide polymorphisms (SNPs) by fluorescence polarization detection.²⁴ Since the different T_m for a perfect match between DNA and LNA, and for LNAs a single-nucleotide mismatch is larger than DNAs, single-nucleotide mismatch discrimination is better for LNAs.²⁵ Scanning related SNPs in the genetic code help researchers diagnose many diseases, for example Orum detected the factor V Leiden mutation in 1999.²⁵

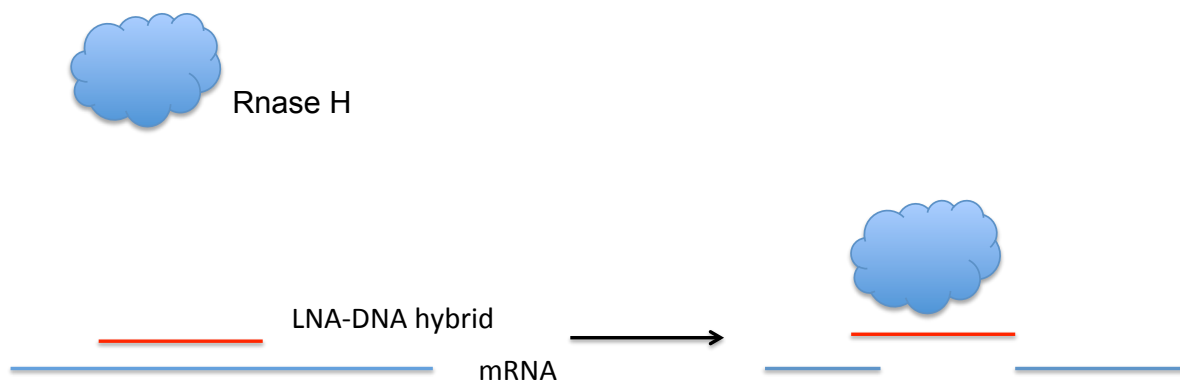


Figure 5. Rnase H can be activated by an LNA-DNA hybrid¹⁷

In morpholino oligonucleotides (MOs) the natural sugar ring is replaced by the 6-member morpholine ring. These analogs also show great promise for antisense applications.²⁶ MOs are cost-effective since they can be synthesized easily by starting with available inexpensive ribonucleosides. Phosphorodiamidate-linked morpholino oligonucleotides (**Figure 6**) with a nonionic backbone have attracted much more attention due to their high aqueous solubility, efficient resistance to nucleases, high affinity binding to RNA, and high chemical stability.²⁷

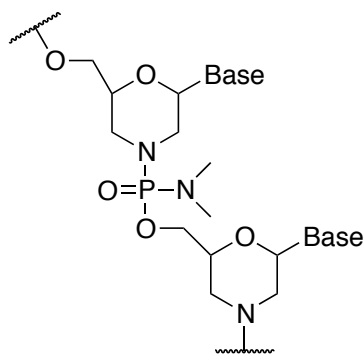


Figure 6. Chemical structure of a morpholino oligonucleotide²⁷

MOs were first introduced as genetic inhibitors in embryos. Several studies have shown that MOs can be injected into zebrafish²⁸ or *Xenopus* embryos,²⁹ interfering with gene expression in a sequence-specific manner and producing phenotypic effects during the early period of development. MOs are being used to selectively target zygotic RNAs when coexist with maternal RNA transcribed by the same gene code.¹ Even though there still exist some drawbacks in most injection experiments, MOs speed up the pace of developmental biology.

Other nucleic acid mimics like GNA (Glycol Nucleic Acid),³⁰ TNA (Threose Nucleic Acid),³¹ UNA (Unlocked Nucleic Acid)³² etc. also have been designed in recent years, however their applications are not as broad as PNA, LNA or morpholino oligonucleotides and still have some drawbacks to overcome. Therefore, highly-effective nucleic acid mimics, widely applicable in diagnostics, therapeutics and related fields are still limited. Under this background, our research group is making efforts in development of novel and advanced nucleic acid mimics.

Chapter 2 Design and Synthetic Efforts Toward a Novel Nucleic Acid Analog

2.1 Designed Novel Nucleic Acid Analogs by Our Group

Our goal is to design novel and improved nucleic acid mimics, binding to a complementary ssDNA or ssRNA. The usual approach retains the natural nucleobases of DNA/RNA and replaces the backbone with novel linker structures designed by computational design methods. The design process follows two steps: (1) define the desired relative position of bases; (2) identify the structures of the backbone via searching a virtual molecular library using a computer program.

In previously work, the following 4 structures (**Figure 7**) of nucleic acid analogues which connect the base linked furans with suitable linkers were designed by CAVEAT's database.³³ The approach to obtain these 4 structures was designed by starting with a nucleobase connected to a furan ring.

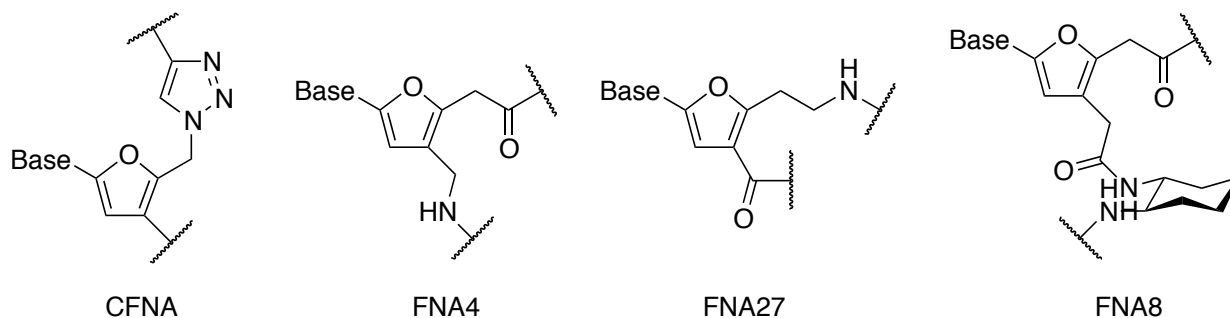


Figure 7. Monomer structures of four furan based backbone

Another approach of synthesizing the novel nucleic acid mimics is introduced in Fig. 8. Upon rotating the P-O5 and C5-C4 bonds of the local backbone conformation of the natural helical DNA or RNA, the face to face distance between sequential nucleobases was elongated from 3.4Å (an ideal distance for favorable π -stacking) to 7.4Å (**Figure 8**).

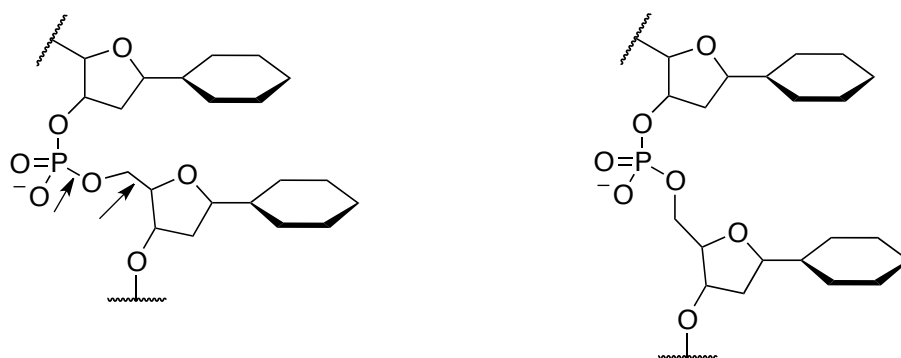


Figure 8. Natural and elongated nucleic acid structures

The increased distance allows another aromatic ring to be inserted into the space between each pair of nucleobases, introducing additional π -stacking between the inserted aromatic ring and nucleobases to enhance binding stability. Therefore, we explored to design a structure that could bind to the rotated and elongated complementary DNA or RNA strand. This designed structure would have natural nucleobases to base-pair with the bases of the targeted DNA or RNA strand and a large “sandwich” base that sits between the two base pairs above and below, all connected by a somewhat rigid backbone (**Figure 9**). And 3-D picture of the “sandwich” base nucleic acid complex was shown in Fig.10.

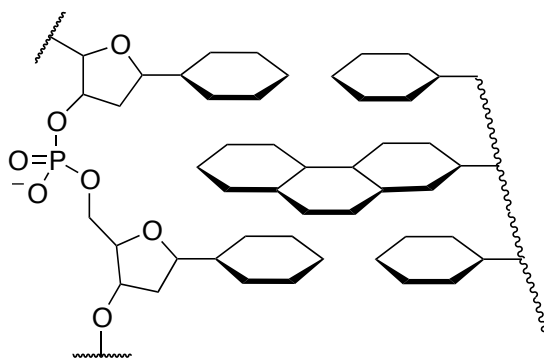


Figure 9. Model of our nucleic acid analog bind with elongated nucleic acid

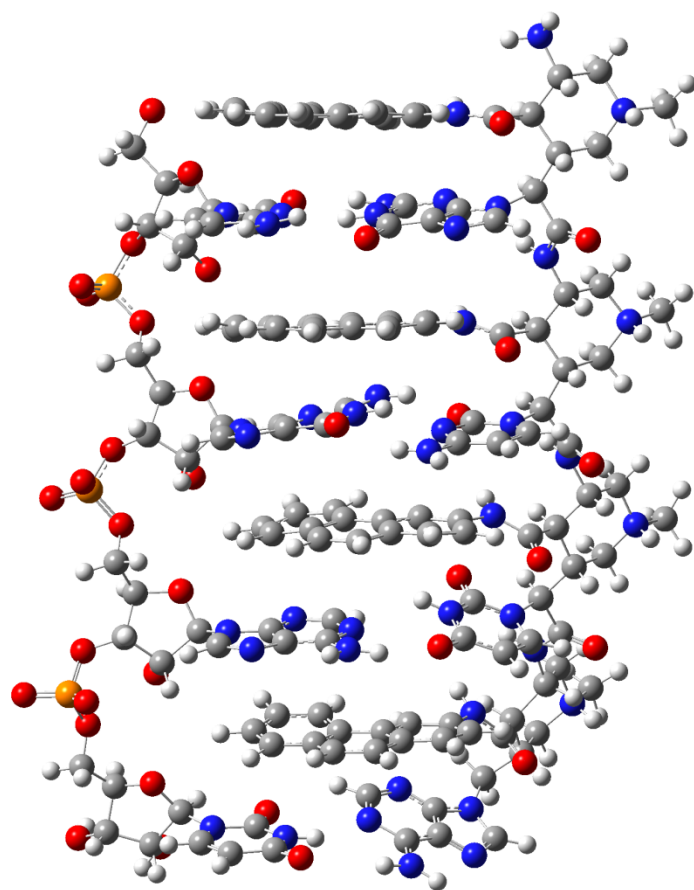


Figure 10. 3-D figure of the “sandwich” base nucleic acid complex

By using HostDesigner, we designed the following 6 structures (**Figure 11**).

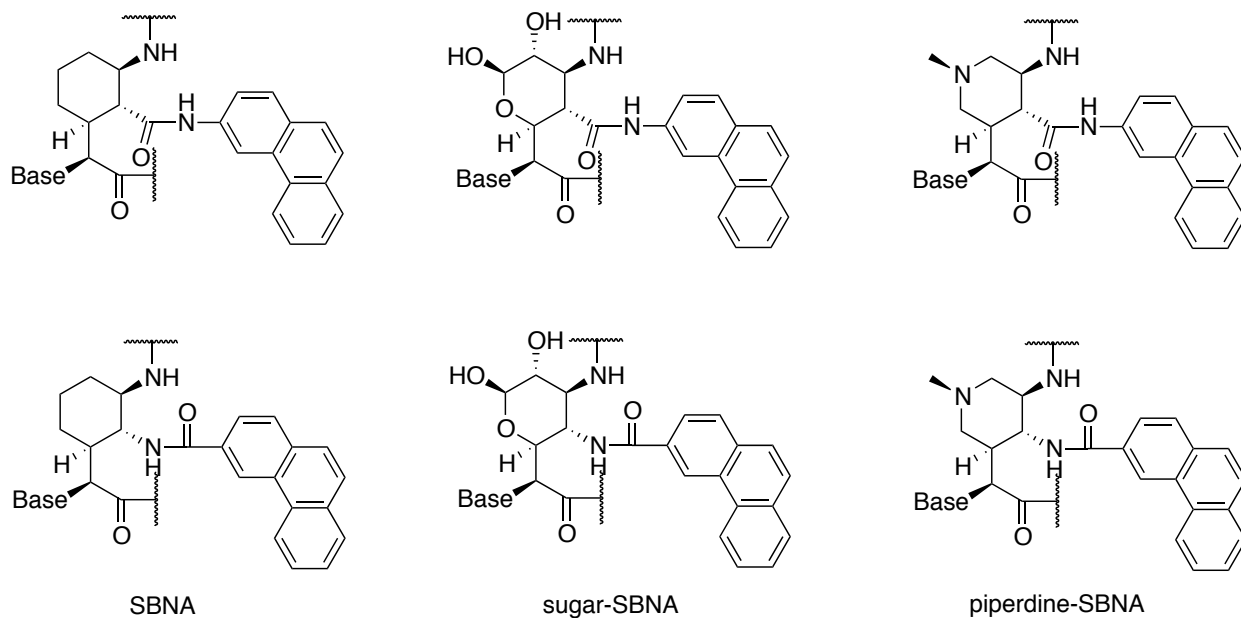


Figure 11. Repeating unit structures of “sandwich” base nucleic acid designs

We employed MD (Molecular Dynamics) simulations and MM/GBSA (Molecular Mechanics/Generalized Born Surface Area) binding energy estimates for our designed nucleic acid mimics and the furan based analogs in Fig. 7, to estimate the binding affinity and stability of binding molecules. The results predict that the SBNA series have the best properties for binding to the complementary DNA or RNA strand. The binding properties of the furan analogs were not as good as SBNA and natural DNA. Energy calculations and visualization of trajectory predict that the SBNAs should bind extremely well to RNA. Thus we have undertaken the synthesis of the SBNA structure, and put the furan based analogs as a second priority.

2.2 Synthetic Background

We selected the piperidine-SBNA structure with a 2-methoxy ethyl group attach to N instead of a methyl group as in the modeling stage for synthesis. The methoxy group should increase solubility to the molecule, and 2-methoxyethyl amine was available in our lab. Fig. 12 shows the structure of our designed molecule.

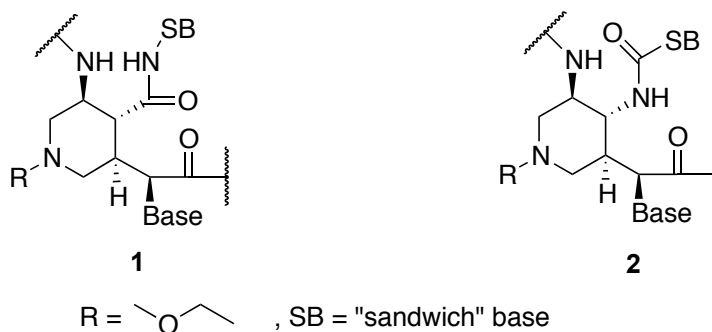


Figure 12. Designed structures of "sandwich" base nucleic acids

The structure has four stereocenters on the piperidine as shown in **Figure 13**. Forming the piperidine ring with consecutive R, R, S, R stereocenters as shown is the key step in the synthesis of this monomer.

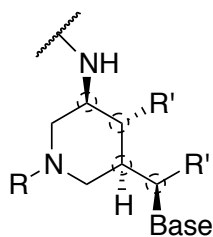
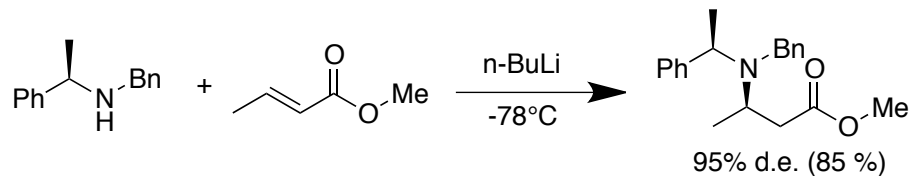


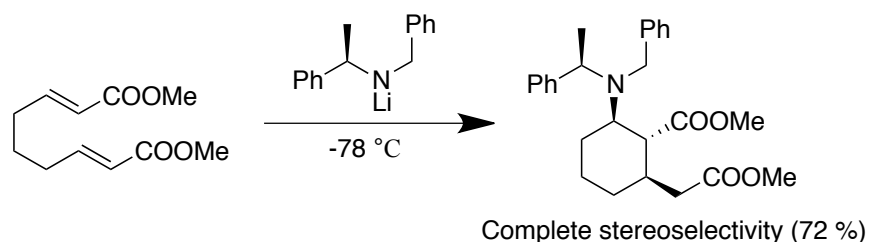
Figure 13. Structure of "sandwich" base nucleic acid with four stereocenters

High diastereoselectivity and good yield has been observed in the Michael addition reaction between lithium amides and alkyl crotonates as shown in **Scheme 1**.³⁴



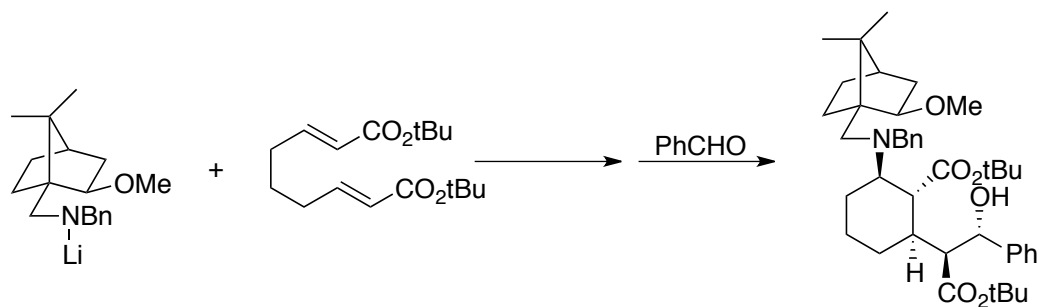
Scheme 1. Michael addition reaction between (R)-N-benzyl-1-phenylethylamine and methyl crotonate gives great stereoselectivity and good yield

It also has been reported that the use of homochiral lithium amides to initiate the intramolecular tandem conjugate addition-cyclisation of diendioate esters generates the cycloproducts with high stereoselectivity as shown in **Scheme 2**.³⁵



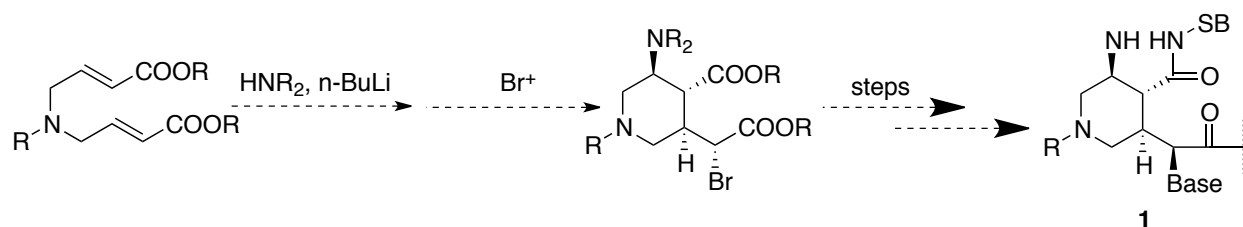
Scheme 2. Tandem Michael addition of the lithium amide to a diendioate ester with complete selectivity

After quenching the reaction with 10 % ammonium chloride solution, three stereocenters are formed.³⁶ Another literature reported that quench the reaction mixture with benzaldehyde follows the tandem Michael addition, five stereocenters can be generated as shown in **Scheme 3** using a different chiral lithium amide nucleophile.³⁷



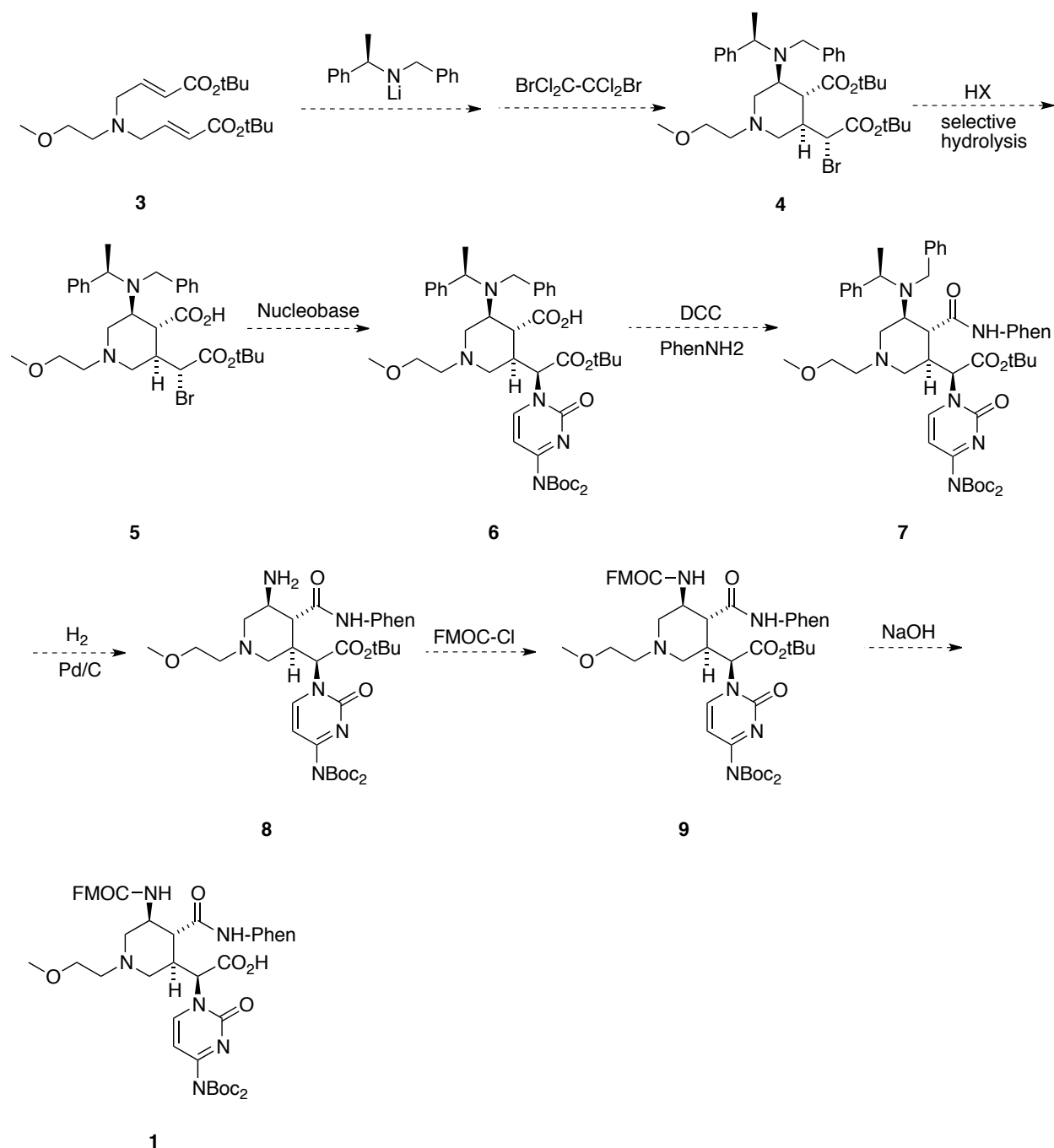
Scheme 3. A product with five stereocenters can be formed through tandem Michael addition

Since the structures above are similar to our designed monomer, we considered using the same synthetic strategy to obtain our designed product with four consecutive stereocenters on the piperidine backbone. The key step in our synthetic route is shown in **Scheme 4**.



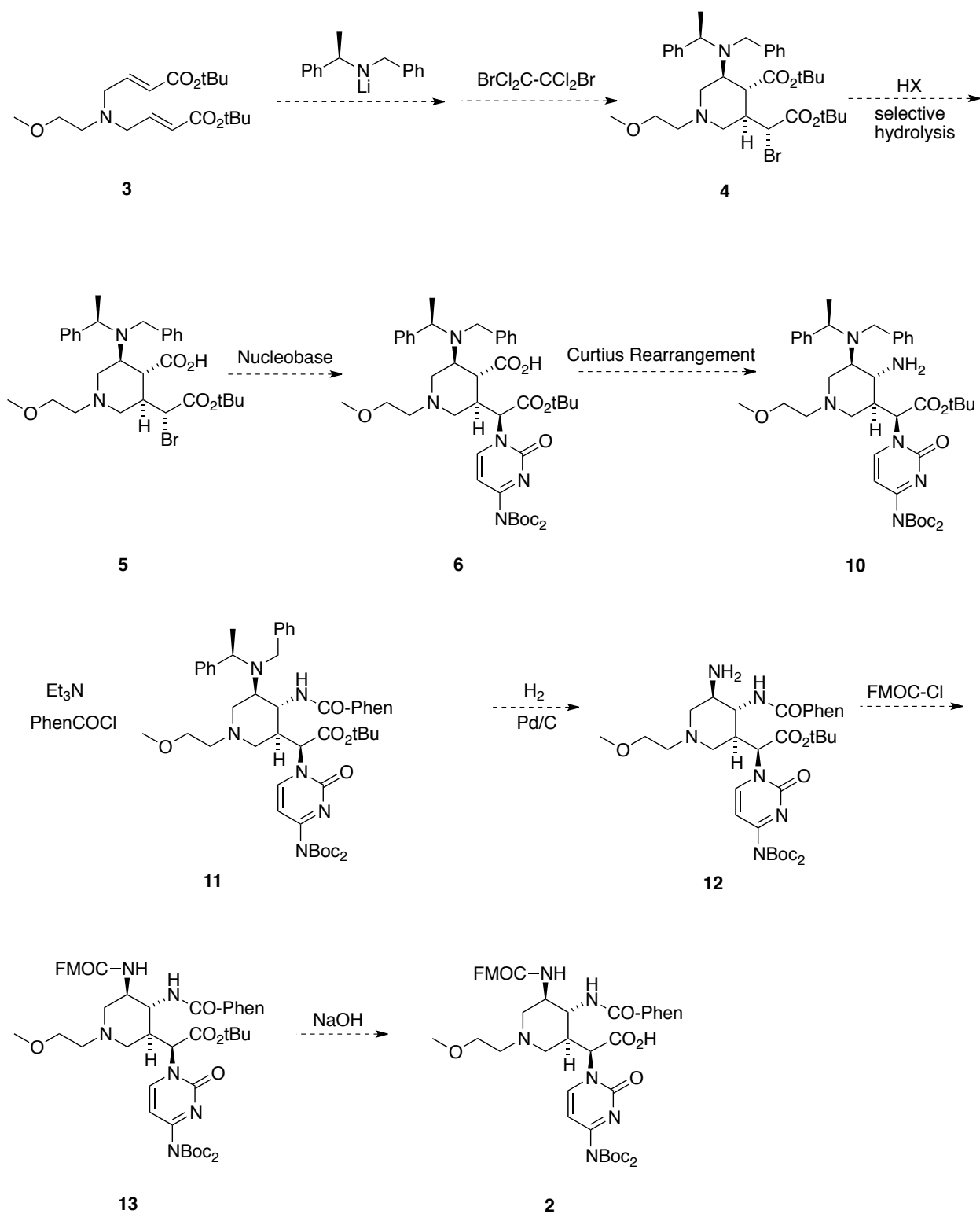
Scheme 4. Synthesis of piperidine backbone

One potential synthetic route for molecule **1** based on this sequential Michael addition approach is shown in **Scheme 5**. A key issue in this route is whether the selective ester hydrolysis of **4** as proposed can be achieved.



Scheme 5. Synthesis of the amine form of "sandwich" base nucleic acid

We also consider the isomeric product **2**, in which the orientation of the amide bond connecting the sandwich base to the piperidine ring is reversed. The difference between synthetic route for molecule **2** and the above one is the addition of a Curtius rearrangement reaction that transforms the upper ester to an amine group (**Scheme 6**).



Scheme 6. Synthesis of the carboxylic acid form of "sandwich" base nucleic acid

The synthesis of our designed molecule should consist of two parts: the synthesis of the “sandwich” base and the synthesis of the piperidine backbone. I first worked on the synthesis of the two forms of “sandwich” base (**Figure 14**).

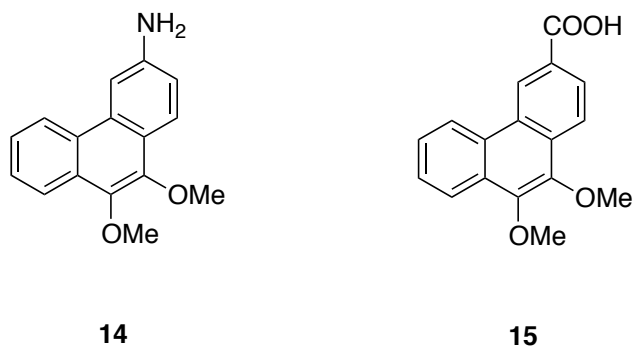
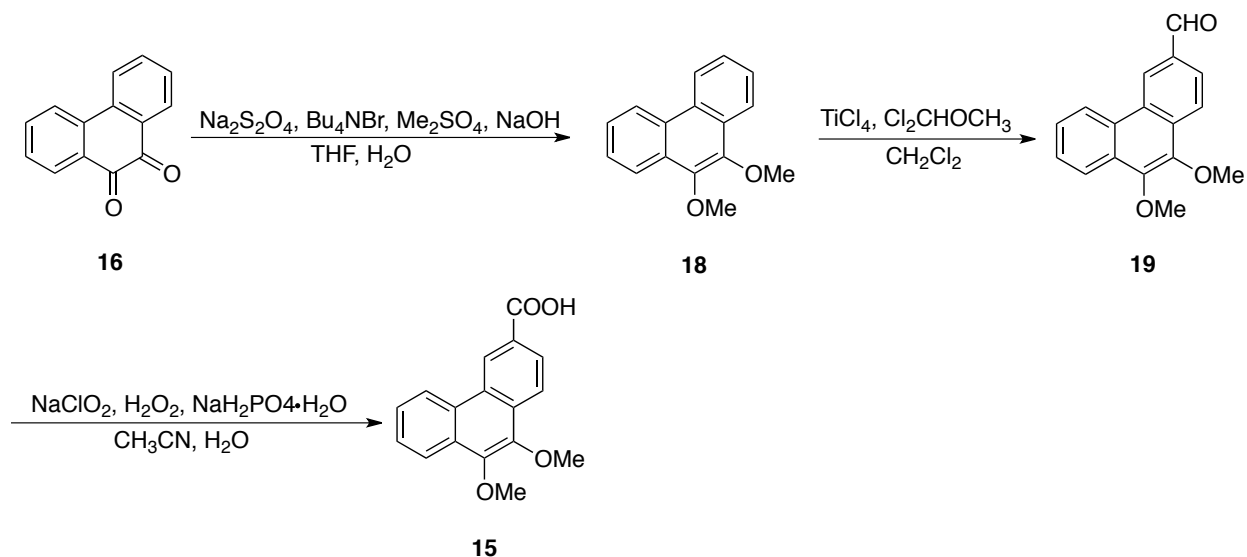


Figure 14. Structures of the amine form and carboxylic acid form of the “sandwich” base

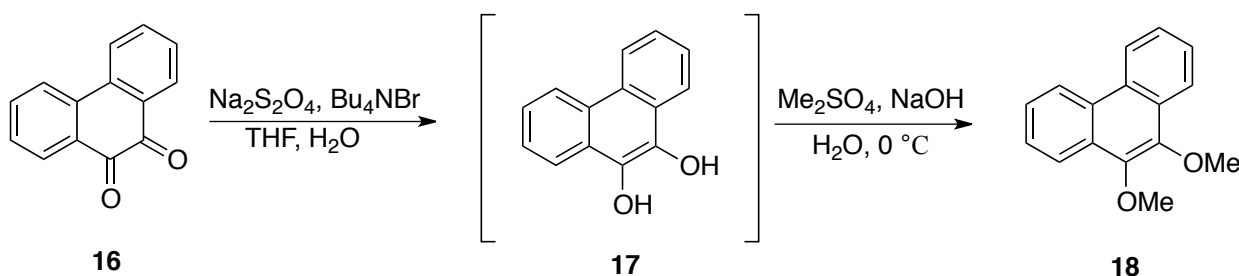
2.3 Synthesis of the Carboxylic Acid Form of “Sandwich” Base

I started with synthesizing the carboxylic acid form of “sandwich” base **15** from the commercially available 9,10-phenanthrenequinone **16** (**Scheme 7**).



Scheme 7. Synthesis of the carboxylic acid form of “sandwich” base

First, the known compound **18** was prepared following literature procedures.³⁸ Sodium dithionite was used as a reductive agent to reduce **16** to an intermediate **17**, which was not isolated. Then dimethyl sulfate was used to methylate the two alcohol groups to methoxy groups to get 9,10-dimethoxyphenanthrene **18** (**Scheme 8**).³⁸



Scheme 8. Synthesis of 9,10-dimethoxyphenanthrene

The mixture of 9,10-phenanthrenequinone, sodium dithionite and tetrabutylammonium bromide (Bu_4NBr) dissolved in a mixture of tetrahydrofuran (THF) and water was shaken. Bu_4NBr worked as a phase transfer catalyst, solubilizing the salts into the organic phase and accelerating the reaction. The color of the solution was changed in a few minutes that showed the intermediate **17** was formed. Following the addition of dimethyl sulfate, sodium hydroxide aqueous solution and ice, the mixture was shaken continuously. During this process, the color changed variously. After quenching the reaction, TLC (Thin Layer Chromatography) (heptane: acetone = 19: 1) only showed two spots, one was the starting material **16** and one was the less polar methylated product (**Figure 15**). No side reaction was observed. The yield of product **18** was 89 %.

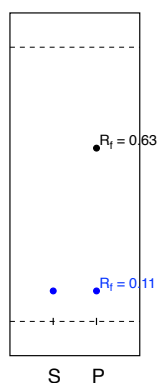
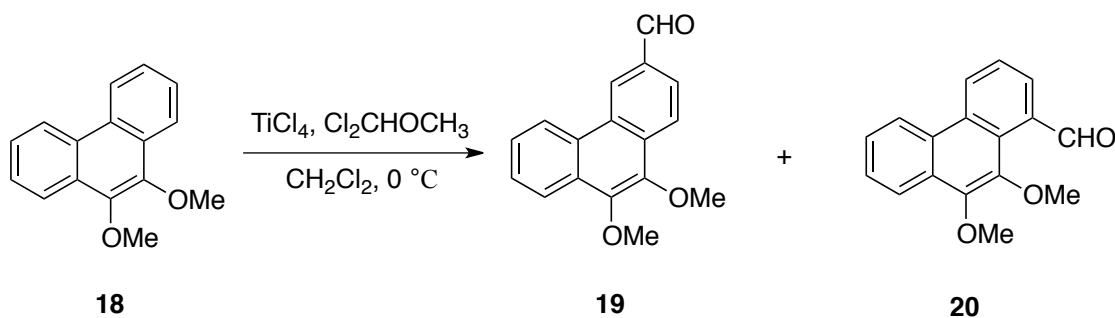


Figure 15. TLC plate of methylation of 9,10-phenanthrenequinone
(S= starting material, P= product)

Compound **18** was used as the substrate for the Rieche formylation reaction shown in scheme 9. This reaction is a type of formylation reaction named after Alfred Rieche in 1960.³⁹ This reaction of **18** has been reported to form the mixture of isomers **19** and **20** (**19**: **20** = 3: 1 from the literature) as shown.⁴⁰ To add a formyl group on the aromatic ring, dichloromethyl methyl ether was used as the formylation reagent, while titanium (IV) chloride was used as the catalyst.⁴⁰



Scheme 9. Formylation of 9,10-dimethoxyphenanthrene

To a solution of the substrate **18** in chloromethane, the catalyst titanium (IV) chloride was added at 0 °C, followed by dropwise addition dichloromethyl methyl ether. The reaction mixture was warmed up to room temperature, stirred for 3.5h and poured into ice water. Four spots were

observed on TLC (heptane: acetone = 19: 1), including a spot of starting material **18**, a spot of large polar impurity, and two very close spots (**Figure 16 left**). Separation was attempted by column chromatography. Unfortunately, the two products with very similar polarity could not be separated. The H-NMR spectrum showed that the resultant product was a crude mixture of two regioisomeric aldehydes **19**, **20** (**19**: **20** = 3: 10). 9,10-Dimethoxyphenanthrene-3-carbaldehyde **19** is our desired product in this step. This step yields the mixture of aldehydes in a combined yield of 65%. Extending the reaction time from 3.5h to 6.5h increased the total yield to 75%.

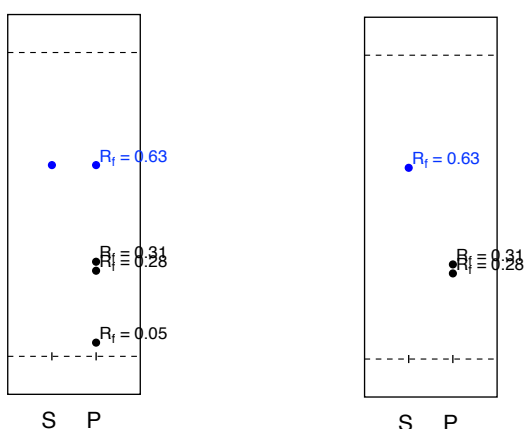
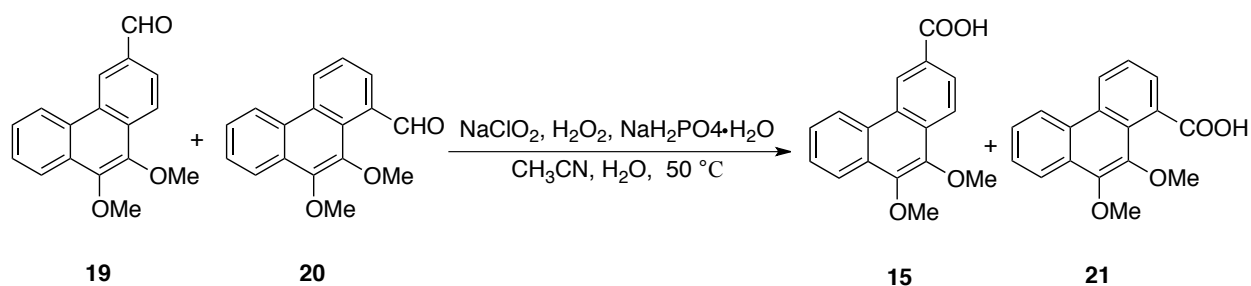


Figure 16. TLC plates of formylation of 9,10-dimethoxyphenanthrene

After not being able to separate the isomeric aldehyde products, we decided to oxidize the mixture of aldehydes to the carboxylic acids as the last step in the synthesis and then attempt separation of the carboxylic acid isomers. Sodium chlorite and hydrogen peroxide were used as oxidizing agents following a general procedure for oxidation of aromatic aldehydes (**Scheme 10**).⁴¹



Scheme 10. Oxidation of mixture of dimethoxyphenanthrene aldehydes

In a monosodium phosphate-buffered aqueous acetonitrile solution, the regioisomeric aldehydes, hydrogen peroxide, and sodium chlorite were stirred for 1h at 50 °C. The reaction was quenched and the resultant product was analyzed by TLC (heptane: acetone = 4: 1). Two close spots appeared on the TLC plate with greater polarity than the aldehydes (**Figure 17**). Separation of these two products was also attempted by column chromatography, and they had been separated successfully. The H-NMR spectrum demonstrated that these two products were the two regioisomeric carboxylic acids (**15, 21**) corresponding to the two regioisomeric aldehydes (**19, 20**) respectively. No side reaction was observed. Based on the content of starting material, each carboxylic acid yielded 90 %.

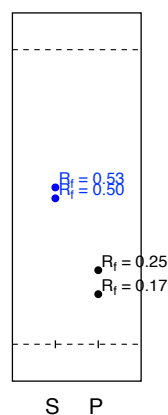
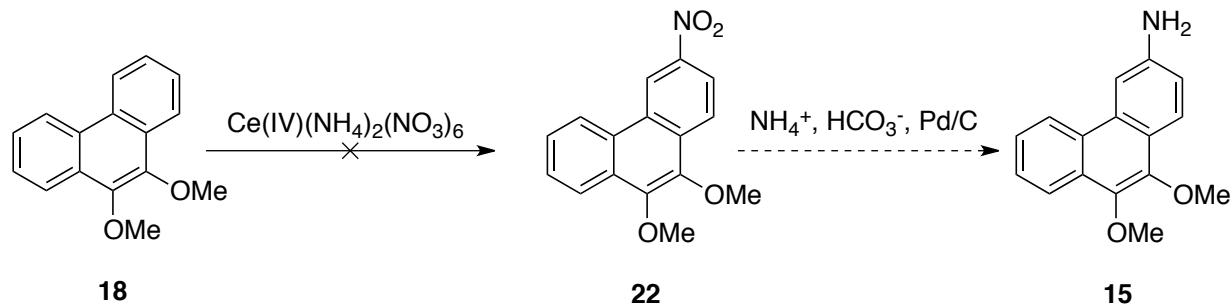


Figure 17. TLC plate of the oxidation reaction of 9,10-dimethoxyphenanthrene aldehydes

2.4 Synthesis of the Amine Form of “Sandwich” Base

Several strategies were attempted to obtain the amine form of the “sandwich” base from the dimethoxyphenanthrene **18**, though most of them failed.

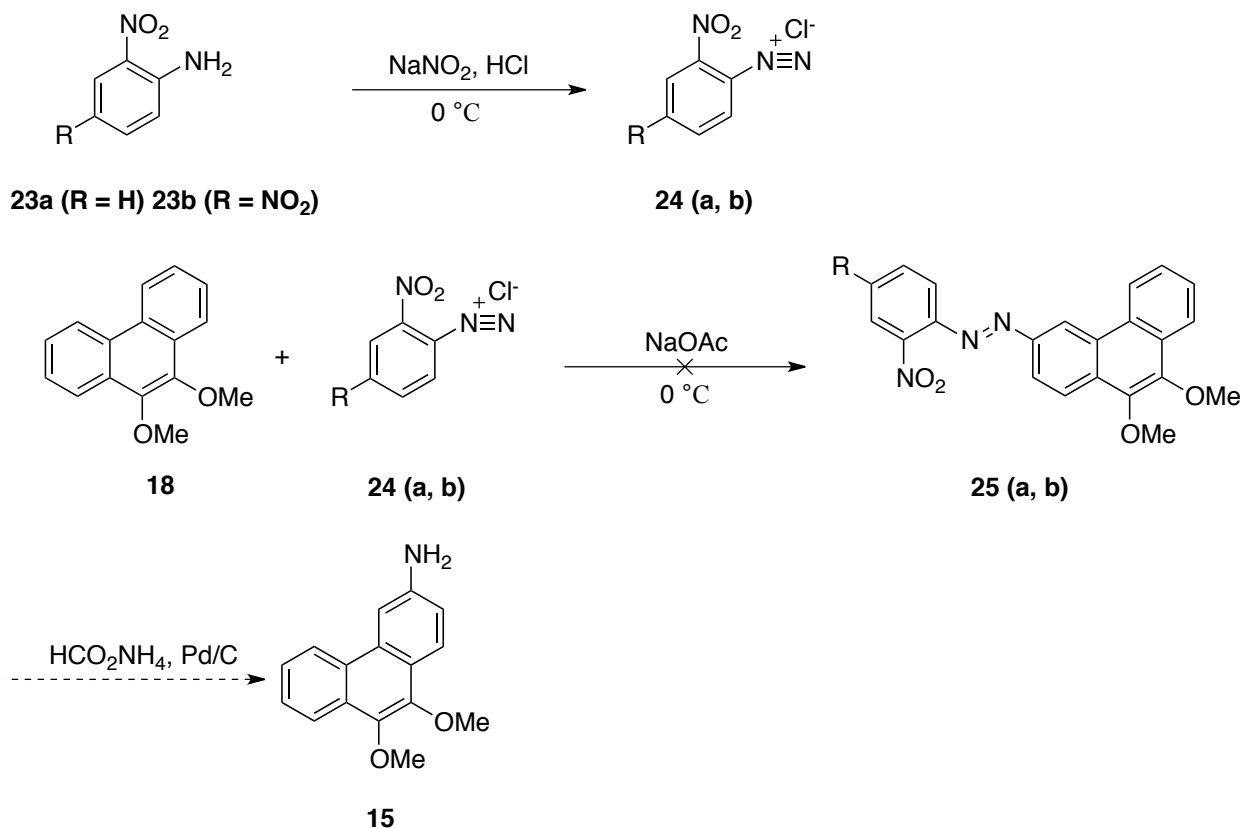
First, a method which uses silica gel-supported cerium (IV) ammonium nitrate for controlled oxidative nitration of some naphthalene derivatives has been reported.⁴² Thus we designed an oxidative nitration reaction of 9,10-dimethoxyphenanthrene **18** to obtain a 9,10-dimethoxy-3-nitrophenanthrene **22**. Then a reducing agent could be used to reduce the nitro group to an amine group, to obtain the amine form of “sandwich” base (**Scheme 11**).



Scheme 11. Attempted oxidative nitration of 9,10-dimethoxyphenanthrene

The oxidative reaction occurs directly on the column according to the reference.⁴² 9,10-dimethoxyphenanthrene was dissolved in acetonitrile, added dry silica gel and mixed. Cerium (IV) ammonium nitrate was also dissolved in acetonitrile, added dry silica gel and mixed. Each was dried separately on a rotary evaporator. The two dry masses were mixed and applied to a dry silica gel column. The column was eluted with hexane/benzene mixtures. One spot appeared on TLC from elution with 4:1 (hexane: benzene). It was 9,10-phenanthrenequinone that demonstrated from H-NMR spectrum. The percentage of benzene in the eluent was increased continually, but still only 9,10-phenanthrenequinone was obtained. Thus other methods were tried.

The second approach started by a diazotization reaction of commercially available *o*-nitroaniline **23a** to get the corresponding unstable diazonium salt **24a**. 9,10-dimethoxyphenanthrene then reacted with **24a** in an attempt to form compound **25a**.⁴³ A reductive reaction would then be used to get the amine form of the “sandwich” base **15** (Scheme 12).



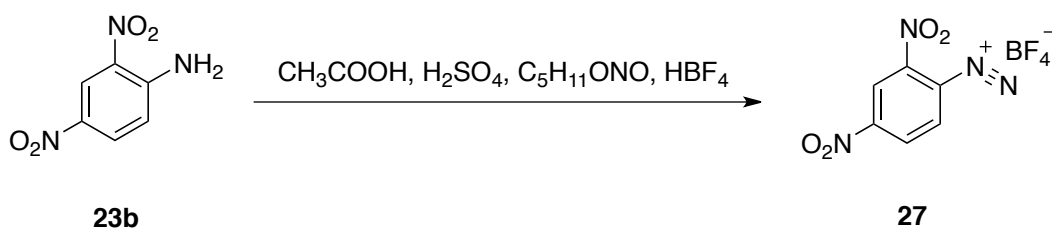
Scheme 12. Diazotization of 9,10-dimethoxyphenanthrene

o-Nitroaniline reacted with nitrous acid, prepared by sodium nitrite and hydrochloric acid, at $0\text{ }^\circ C$ since the obtained diazonium compound **24a** was very unstable. Following addition of sodium acetate and 9,10-dimethoxyphenanthrene, the solution was stirred for 10h at $0\text{ }^\circ C$. The reaction was monitored every 2 hours, however, again only the reactant 9,10-dimethoxyphenanthrene was observed. I theorized a possible reason for failure of the reaction.

Because of the instability of the diazonium compound **24a**, it was not sufficiently reactive during the reaction. In order to get a more reactive diazonium compound, we introduced another nitro group on the aniline. 2,4-Dinitroaniline was used as the starting material in the same procedure described above. Unfortunately, we still did not get the azo compound **25b**, but only the reactant 9,10-dimethoxyphenanthrene was observed by both TLC and H-NMR.

We suspected the diazonium salts **24a** and **24b** may have not been formed. Thus we changed the reagents for the diazotization reaction of 2,4-dinitroaniline. 2,4-Dinitroaniline was dissolved in sulfuric acid at 0 °C followed by addition of nitrosylsulfuric, which was prepared from sodium nitrite and sulfuric acid, and finally phosphoric acid was added.⁴⁴ After stirring the reaction mixture for 1.5 h, urea was added, followed by addition of 9,10-dimethoxyphenanthrene at 0 °C. The reaction was monitored every 2 hours by TLC. I observed two spots on the plate, including the spot of 9,10-dimethoxyphenanthrene. The polarity of the other spot was higher than 9,10-dimethoxyphenanthrene from TLC. However, the other spot was an undesired product demonstrated by H-NMR. The H-NMR spectrum indicated reaction of the aniline occurred, as the chemical shift of two of the three aromatic hydrogens shifted to the higher values.

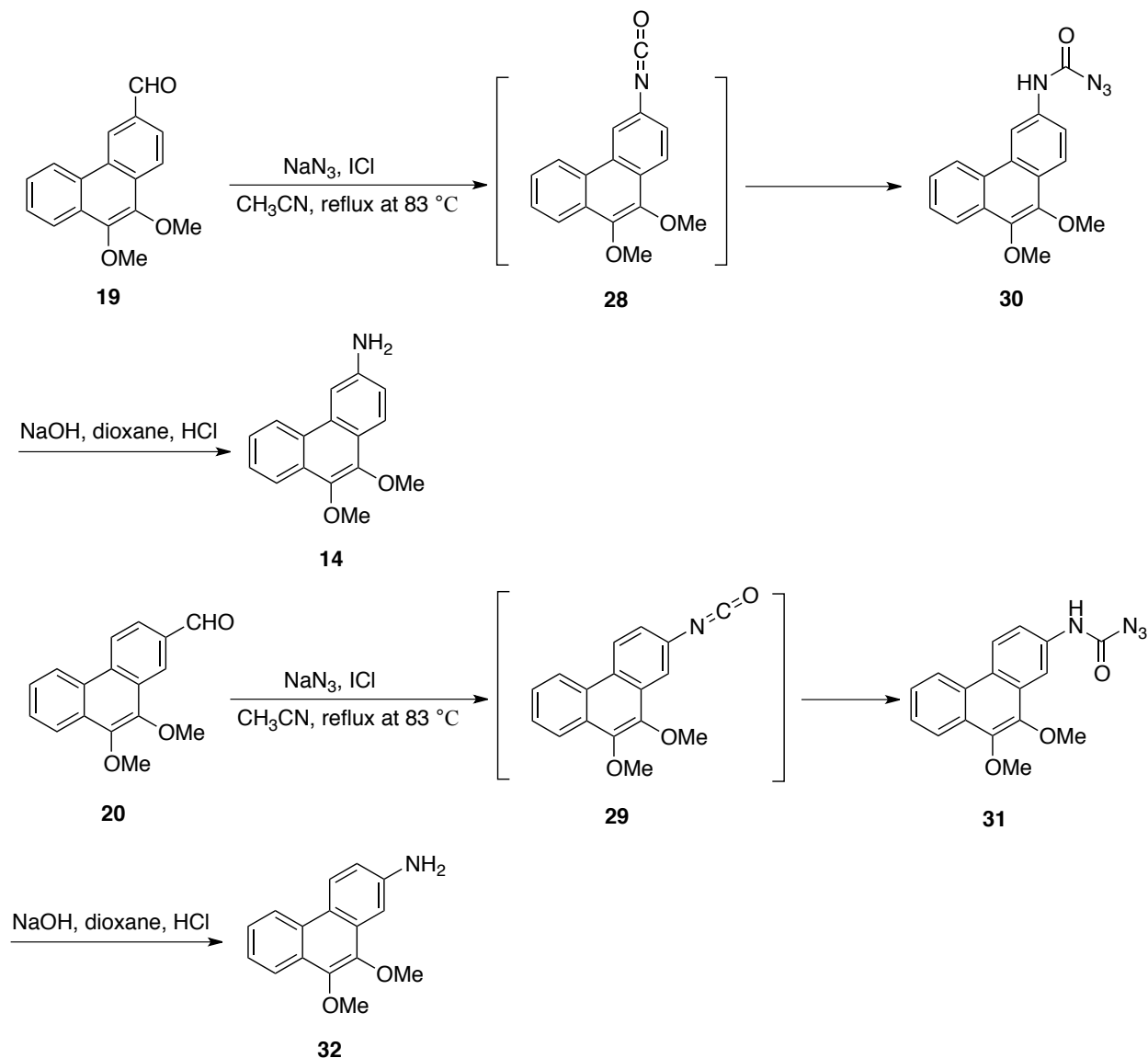
In all the diazotization reactions described above, diazonium salts were not isolated and thus it was unclear if they were ever formed. Thus we found a way to isolate the diazonium compounds as tetrafluoroborate salts (**Scheme 13**), which are stable at room temperature.



Scheme 13. Diazotization of 2,4-dinitroaniline

This time glacial acetic acid and sulfuric acid were used to dissolve 2,4-dinitroaniline at 120 °C followed by rapid cooling. Isopentyl nitrite was then added to form the diazonium salt. Finally tetrafluoroboric acid was added to obtain the stable and storable 2,4-dinitrobenzenediazonium tetrafluoroborate⁴⁵ which could react with the phenanthrene in the next step. In the first trial, a problem appeared during the operation that some solid was precipitated when the solution was cooling rapidly, but I still followed next step. And the second time I did not cool the acid solution dissolved 2,4-dinitroaniline, added isopentyl nitrate directly, and followed the next step. These two trials got the same results that one major spot and several very weak spots were shown on the TLC plate. H-NMR spectrum shown the major spot was an undesired product, and other weak spots were impurities.

After several failures, we came up with another idea that the amine “sandwich” base could be obtained directly from the aldehydes we obtained previously. Aromatic aldehydes are known to react with iodine azide at room temperature to form acyl azides.⁴⁶ If the reaction is performed at reflux, a Curtius rearrangement occurs and carbamoyl azides are formed.⁴⁶ Hydrolysis of the carbamoyl azides could form our designed amine form of the “sandwich” base (**Scheme 14**).⁴⁶



Scheme 14. Synthesis of the amine form of “sandwich” base starting from dimethoxyphenanthrene aldehydes

For the azidonation reaction, the radical reagent iodine azide was first obtained by sodium azide and iodine monochloride in acetonitrile at low temperature.⁴⁶ Then the mixture of two aldehydes was added into the solution, and refluxed the reaction mixture for 4h. TLC (heptane: acetone = 9: 1) showed two major new spots and very weak spots of the aldehydes (**Figure 18**). By H-NMR, we identified the less polar product as the carbamoyl azide of aldehyde **19** and the more polar product as the carbamoyl azide of aldehyde **20**. The desired product **30** and the

isomer **31** were successfully separated by column chromatography. Based on the content of starting material, each carbamoyl azide yielded 88 %.

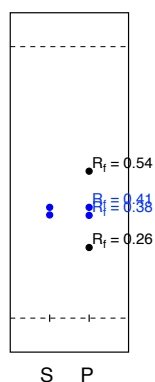


Figure 18. TLC plate of azidation of 9,10-dimethoxyphenanthrene aldehydes

To avoid the possibility of wasting compound **30**, the hydrolysis step was first attempted on compound **31**. Hydrolysis of carbamoyl azide **31** by sodium hydroxide formed carbamoyl acid immediately and after hydrochloric acid workup the amine. One spot was shown on the TLC plate (heptane: acetone = 9: 1) (**Figure 19 left**). H-NMR indicated that this product was the amine **32** indeed and the hydrolysis reaction was feasible. Thus our desired carbamoyl azide **30** was hydrolyzed by same procedure, and we obtained our desired amine form of the “sandwich base” **15** successfully (**Figure 19 right**). The yield of this hydrolysis step was 81%.

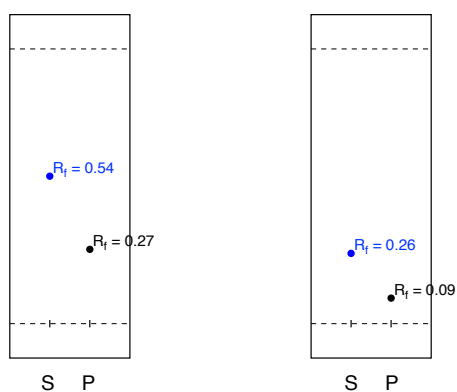
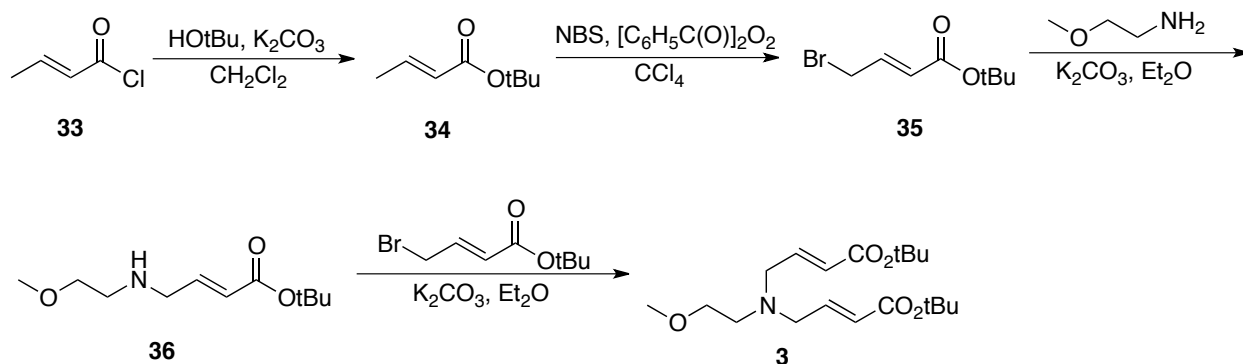


Figure 19. TLC plates of hydrolysis of carbamoyl azides

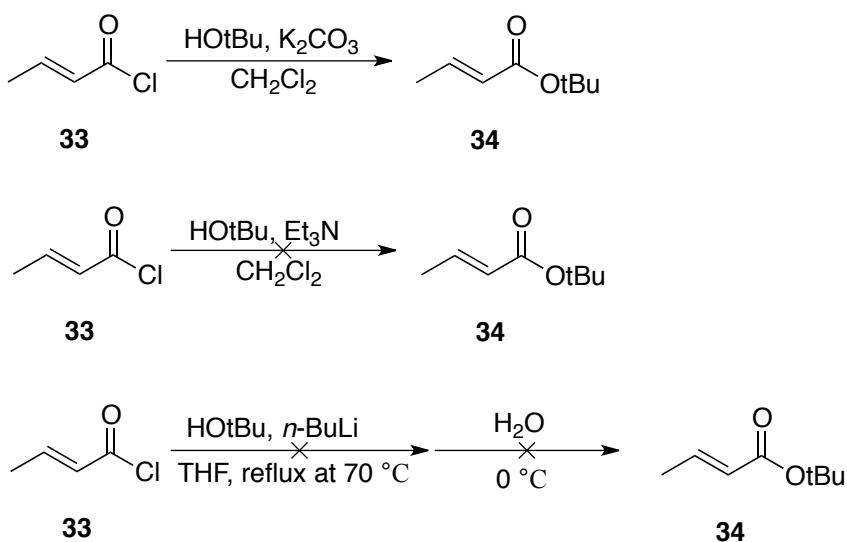
2.5 Synthesis of the Piperidine Backbone

After synthesizing the two forms of “sandwich” base successfully, we then focused on the backbone part. The synthesis of substrate **3** in **Scheme 5** was attempted as shown in **Scheme 15**.



Scheme 15. Synthetic route of the substrate diester

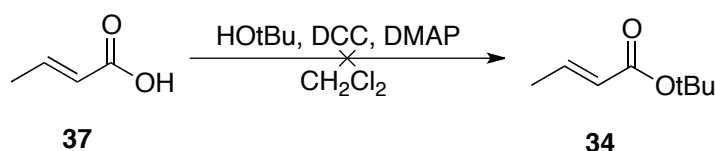
Several strategies were explored to synthesize the *t*-butyl crotonate **34**.⁴⁷ Acylation of *t*-butyl alcohol with crotonyl chloride was attempted under alkaline conditions. Potassium carbonate, triethylamine and *n*-butyl lithium⁴⁷ were used as base in three procedures (**Scheme 16**).



Scheme 16. Trials for synthesis of *t*-butyl crotonate

These reactions all gave the hydrolysis product of crotonyl chloride. Reaction with n-butyl lithium as base gave another undesired product. Only the reaction with potassium carbonate as base gave any of the desired product *t*-butyl crotonate, and this reaction gave product in only 9 % yield.

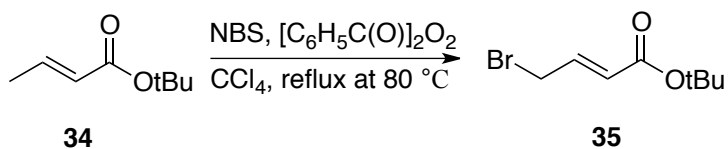
Next a DCC coupling reaction of crotonic acid with *t*-butyl alcohol with 4-dimethylaminopyridine (DMAP) as catalyst and base was attempted (**Scheme 17**).



Scheme 17. DCC coupling reaction for synthesis of *t*-butyl crotonate

This strategy got the unreacted crotonic acid and an intermediate product that formed by crotonic acid and DCC through the results of H-NMR spectrum. Finally, we bought the commercially available *t*-butyl crotonate as the starting material for further reactions.

A free radical reaction was used to form the *t*-butyl- γ -bromo crotonate **35**. This reaction used *N*-bromosuccinimide (NBS) in a CCl₄ solution of *t*-butyl crotonate, with benzoyl peroxide as a radical initiator (**Scheme 18**). Thus, *t*-butyl- γ -bromo crotonate **35** was prepared directly with procedure from literature.⁴⁷



Scheme 18. Synthesis of *t*-butyl- γ -bromo crotonate

The reaction was stirred overnight under reflux. Monitoring the reaction by TLC, we observed two spots on TLC (heptane: acetone = 19: 1) (**Figure 20**) including the starting material spot. The other spot was the desired bromination product of *t*-butyl crotonate. No side reaction was observed and the yield was 82%.

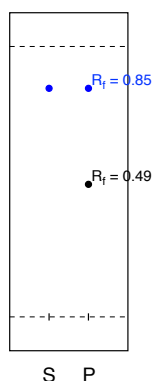
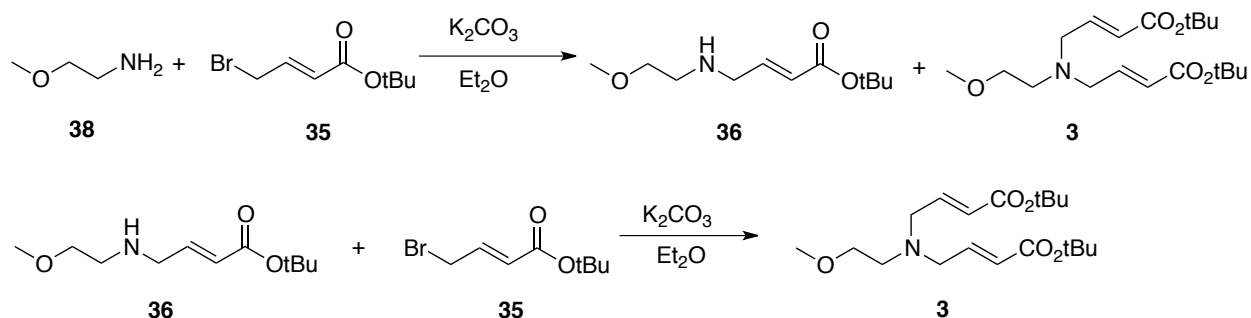


Figure 20. TLC plate of bromination of *t*-butyl crotonate

An alkylation reaction between 2-methoxyethylamine **38** and **35** with potassium carbonate base yielded a mixture of monoalkylated amine **36** (47 %) and tertiary amine **3** (35 %) (**Scheme 19**). The TLC result (heptane: acetone = 4:1) is shown in **Figure 21 (left)**. A second alkylation reaction between monoalkylated amine **36** and 4-bromocrotonate formed tertiary amine **3** in 56 % yield (**Figure 21 right**) (**Scheme 19**).



Scheme 19. Alkylation of *t*-butyl- γ -bromo crotonate

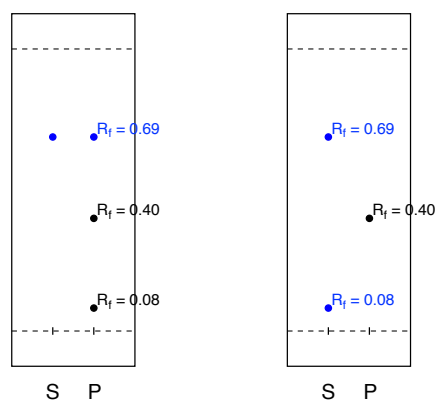
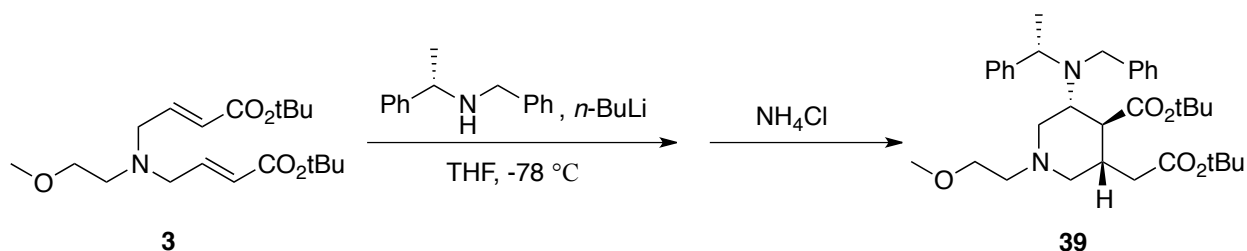


Figure 21. TLC plates of alkylation reactions

We found that a ratio of 2-methoxyethylamine and 4-bromocrotonate of 2:5 gave the highest yield. 4-Bromocrotonate did not react totally, and was recovered and reused. These two alkylation reactions gave an overall yield of **3** of 61%.

After synthesizing substrate **3** successfully, we tried the tandem Michael addition.³⁵ To initially test this reaction, the reaction was quenched with mild acid to form the protonated product **39** rather than the ultimately desired brominated product (**Scheme 20**).³⁶

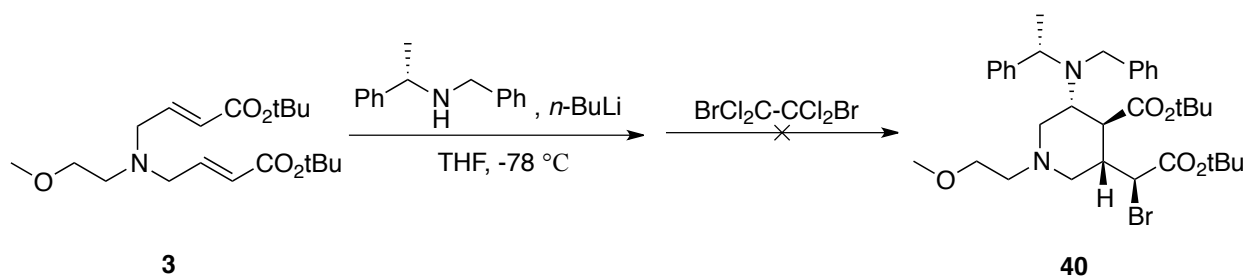


Scheme 20. Tandem Michael Addition of the substrate of diester

First, *n*-butyllithium was added to the THF solution of *S*-(α -methylbenzyl)benzyl amine to form the homochiral lithium (α -methylbenzyl)benzyl amide at -78 °C. Then a solution of **3** was added dropwise at the same temperature, and the reaction was stirred for 2h. The reaction was

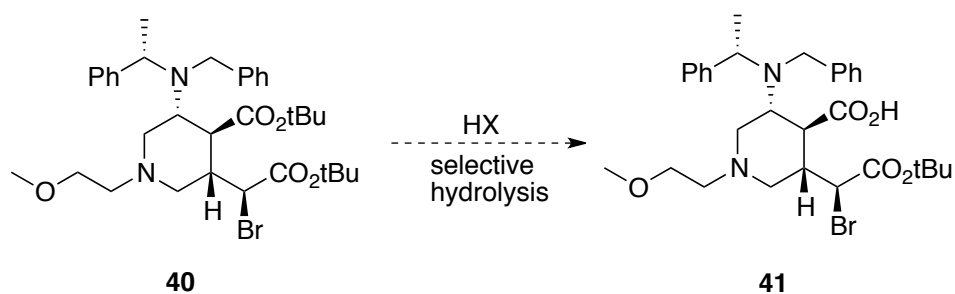
quenched with 10% ammonium chloride and two spots were observed on TLC. One spot was the excess S-(α -methylbenzyl)benzyl amine, the other one was the desired conjugate addition-cyclization product as demonstrated through H-NMR. The yield was 88 %. This success indicated that the tandem Michael addition could be easily applied to our designed molecule. Thus, we could try to introduce the α -bromination step in this reaction.

Instead of quenching with 10% ammonium chloride, we first quenched the reaction with 1,2-dibromotetrachloroethane at $-78\text{ }^{\circ}\text{C}$ for 1h, then quenched again with saturated ammonium chloride (**Scheme 21**).⁴⁸ Unfortunately, the products could not be identified but the H-NMR was not consistent with the desired product.



Scheme 21. Bromination follows tandem Michael Addition of the substrate diester

Because the bromination step was not successful, the key selective hydrolysis step has not been attempted (**Scheme 22**). More work is needed to obtain the desired brominated product **40** before conditions for the selective hydrolysis step can be studied. Another student in the Drueckhammer group is also exploring other routes to the substituted piperidine product.



Scheme 22. Proposed selective hydrolysis of the piperidine backbone

2.6 Conclusion and Future Work

In our study, we worked on the synthesis of a novel “sandwich” base nucleic acid analog. We have successfully synthesized both the carboxylic acid and amine form of the dimethoxyphenanthrene “sandwich” base. A tandem Michael addition had been applied to the synthesis of the substituted piperidine backbone, to obtain the desired product with 3 consecutive stereocenters but without introduction of the bromine to create the fourth stereocenter.

Building the substituted piperidine backbone with 4 consecutive stereocenters is still underway in the Drucekhammer lab. Once bromination on the fourth stereocenter is successful, we will try the challenging step of selective hydrolysis. In the long term, the affinity and selectivity when binding with a complementary strand of our synthesized nucleic acid analog will be evaluated *in vitro*. If results are positive, we will try to transport the nucleic acid analog into cells to detect whether it also hybridizes in cells. This nucleic acid analog may be used as a novel inhibitor in both antisense and antigene strategies *in vivo*.

Chapter 3 Procedures

9,10-dimethoxyphenanthrene (18)³⁸

9,10-phenanthrenequinone (5.20 g, 25 mmol), sodium dithionite (12.88 g, 74 mmol), tetrabutylammonium bromide (2.58 g, 8 mmol) were added to a 250 ml separatory funnel containing a mixture of water (50 ml) and THF (50 ml). The separatory funnel was shaken for 5 min. Dimethyl sulfate (15.5 ml, 0.13 mol), 34 % aqueous sodium hydroxide (25 ml) and 40 g ice were added to the separatory funnel that was shaken for another 5 min. An additional 40 g ice was added. After shaking for another 10 min, ethyl acetate (20 ml) was added and the mixture was shaken continuously. The layers were separated and the aqueous phase was further extracted with ethyl acetate (2 x 20 ml). The combined organic layers were washed with water (3 x 20 ml), 15 % aq. ammonia (2 x 20 ml), water (3 x 20 ml), and brine (20 ml). The solution was dried with anhydrous magnesium sulfate. Solvent was removed via rotary evaporation to obtain an orange oil. The product was purified by column chromatography (heptane: acetone = 19:1) to give **18** (5.30 g, 89 %) as a yellow oil. δ_{H} (300 MHz, CDCl_3), 4.11 (s, 6H), 7.58-7.70 (m, 4H), 8.23-8.31 (m, 2H), 8.62-8.69 (m, 2H). H-NMR data matched the literature value.

Formylation of 9,10-dimethoxyphenanthrene (18)⁴⁰

9,10-dimethoxyphenanthrene (1.19 g, 5 mmol) was dissolved in 25 ml dichloromethane, and titanium (IV) chloride (1.19 g, 6.25 mmol) was added at 0° C. After adding dichloromethyl methyl ether (0.86 g, 7.5 mmol) dropwise into the solution, the reaction mixture was allowed to warm to room temperature. After 1h stirring, ice was added into the solution. The resulting solution was then extracted with dichloromethane (2 x 10ml). The combined organic phases were washed with 5% aqueous sodium bicarbonate solution (15ml), dried with anhydrous magnesium

sulfate and the solvent was removed by rotary evaporation. After purifying via column chromatography (heptane: acetone = 9:1), a pale yellow solid mixture of regioisomeric aldehydes (1 g, 75%) was obtained. The ratio between the two aldehydes as determined by H-NMR integration was 3: 10.

9,10-dimethoxyphenanthrene-3-carbaldehyde (19)

Yield 0.23 g (17.3 %). δ_{H} (300 MHz, CDCl_3), 4.09 (s, 3H), 4.15 (s, 3H), 7.61-7.74 (m, 2H), 8.10 (dd, 1H, $J = 8.7$ Hz, $J = 1.2$ Hz), 8.24-8.32(m, 1H), 8.35 (d, 1H, $J = 8.4$ Hz), 8.70-8.78 (dd, 1H, $J = 6.0$ Hz, $J = 3.3$ Hz), 9.13 (s, 1H), 10.25 ppm (s, 1H), H-NMR data matched the literature value.

9,10-dimethoxyphenanthrene-1-carbaldehyde (20)

Yield 0.77 g (57.7 %). δ_{H} (300 MHz, CDCl_3), 3.97 (s, 3H), 4.15 (s, 3H), 7.61-7.74 (m, 3H), 7.92 (dd, 1H, $J = 7.5$ Hz, $J = 1.2$ Hz), 8.24-8.32(m, 1H), 8.62-8.68 (m, 1H), 8.83 (dd, 1H, $J = 8.4$ Hz, $J = 0.6$ Hz), 11.03 ppm (s, 1H), H-NMR data matched the literature value.

Oxidation of 19, 20 mixture⁴¹

1 g mixture of **19**, **20** (**19**: **20** = 3: 10, 3.76 mmol) was dissolved in a mixture of water (3.5 ml) and acetonitrile (6.5 ml). To the resulting solution was added 30 % aqueous hydrogen peroxide (0.42 ml, 4.14 mmol), sodium chlorite (0.58 g, 6.41 mmol) and sodium phosphate monobasic monohydrate (0.15 g, 1.12 mmol). The mixture was stirred for 1 h at 50° C. The resulting solution was extracted with ethyl acetate (2 x 10ml) and the combined organic layers were dried with anhydrous magnesium sulfate. The product was purified via column chromatography, elution gradient from heptane: acetone = 9:1 to 3:1 to yield two regioisomeric products **15** and **21** as determined by H-NMR.

9,10-dimethoxyphenanthrene-3-carboxylic acid (15)

Yield 0.22 g (90 %), δ_{H} (300 MHz, CDCl_3), 4.10 (s, 3H), 4.15 (s, 3H), 7.64-7.80 (m, 2H), 8.22-8.38 (m, 3H), 8.73-8.82 (m, 1H), 9.48 ppm (s, 1H)

9,10-dimethoxyphenanthrene-3-carboxylic acid (21)

Yield 0.73 g (90 %). δ_{H} (300 MHz, CDCl_3), 4.10 (s, 3H), 4.14 (s, 3H), 7.65-7.80 (m, 4H), 8.27 (d, 1H, $J = 7.8$ Hz), 8.66 (d, 1H, $J = 7.8$ Hz), 8.75 ppm (d, 1H, $J = 7.8$ Hz)

Azidation of 19,20 mixture⁴⁶

Sodium azide (0.78 g, 12 mmol) was dissolved in acetonitrile (12 ml) at 0 °C. Another acetonitrile (12 ml) solution of iodine monochloride (1.30 g, 8 mmol) was added dropwise, followed by addition of a mixture of **19** and **20** (1.06 g, 4 mmol). The reaction mixture was refluxed for 5 h at 83 °C, cooled, and poured into 40 ml water. The solution was extracted with dichloromethane (2 x 40 ml). The organic phase was washed with 5 % sodium thiosulfate solution (40 ml). The solution was dried by anhydrous magnesium sulfate and solvent was removed via rotovap. The product was purified via column chromatography (heptane: acetone = 19: 1) to yield two regioisomeric products **30** (0.26 g) and **31** (0.87 g). Yield 88 % total.

(9,10-dimethoxyphenanthren-3-yl)carbamoyl azide (30)

Yield 0.26 g (88 %). δ_{H} (300 MHz, CDCl_3), 4.06 (s, 3H), 4.07 (s, 3H), 7.50 (t, 1H, $J = 6.9$ Hz), 7.54-7.64 (m, 2H), 8.14 (d, 1H, $J = 9.0$ Hz), 8.20 (d, 1H, $J = 8.1$ Hz), 8.45 (d, 1H, $J = 8.4$ Hz), 8.81 ppm (s, 1H)

(9,10-dimethoxyphenanthren-1-yl)carbamoyl azide (31)

Yield 0.87 g (88 %). δ_{H} (300 MHz, CDCl_3), 4.08 (s, 6H), 7.58 (t, 1H, $J = 8.1$ Hz), 7.62-7.7(m, 2H), 8.16-8.24 (m, 1H), 8.42 (d, 1H, $J = 8.1$ Hz), 8.55-8.65 (m, 2H), 10.70 ppm (s, 1H)

9,10-dimethoxyphenanthrene-3-amine (14)⁴⁶

(9,10-dimethoxyphenanthren-3-yl)carbamoyl azide (**30**) (0.25 g, 0.78 mmol) was added into a mixture of sodium hydroxide (2 ml, 2 M) and dioxane (2 ml). The mixture was stirred for 50 min at room temperature. After addition of hydrochloric acid (6 ml, 2 M), the mixture was stirred for another 50 min. Then sodium hydroxide (2 M) was added into the solution dropwise until the pH value of the solution was 7. It was then extracted with diethyl ether (2 x 20 ml). The combined organic extracts were dried with anhydrous magnesium sulfate and evaporated via rotovap. After purification via column chromatography (heptane:acetone = 9 :1), yielded 0.16 g (81 %) brown oil product. δ_{H} (300 MHz, CDCl_3), 4.03 (s, 3H), 4.08 (s, 3H), 7.05 (dd, 1H, $J = 8.4$ Hz, $J = 1.8$ Hz), 7.46-7.64 (m, 2H), 7.82 (s, 1H), 8.04 (d, 1H, $J = 8.4$ Hz), 8.17 (dd, 1H, $J = 7.8$ Hz, $J = 0.9$ Hz), 8.48 ppm (d, 1H, $J = 8.1$ Hz)

***tert*-butyl crotonate (34)**

tert-Butyl alcohol (0.74 g, 10 mmol) was dissolved in dichloromethane (10 ml). Potassium carbonate (1.38 g, 10mmol) was added into the solution, followed by addition of a dichloromethane (5 ml) solution of crotonyl chloride (1.05 g, 10 mmol) dropwise. The mixture was stirred overnight at room temperature. After filtration, the solution was washed with water (2 x 20 ml), dried, and the solvent was removed under vacuum. The product was purified via column chromatography (heptane:acetone = 9:1) to give a colorless oil 0.13 g (9.2 %). δ_{H} (300

MHz, CDCl₃), 1.48 (s, 9H), 1.85 (dd, 3H, $J = 6.9$ Hz, $J = 1.5$ Hz), 5.77 (dd, 1H, $J = 15.3$ Hz, $J = 1.5$ Hz), 6.87 ppm (m, 1H)

***t*-butyl- γ -bromo crotonate (35)⁴⁷**

N-Bromosuccinimide (6.23 g, 35 mmol) was added into a carbon tetrachloride (50 ml) solution of *tert*-butyl crotonate (5.0 g, 35 mmol). Then benzoyl peroxide (0.05 g, 0.21 mmol) was added. The mixture was stirred and refluxed at 80 °C overnight. The reaction mixture was cooled to room temperature and filtered to remove succinimide. The organic solution was washed with water (3 x 20 ml), dried by anhydrous magnesium sulfate, and evaporated via rotovap under reduced pressure to give a yellow oil. Purification via column chromatography (heptane: acetone = 9: 1), gave a pale yellow oil product 6.34 g (82 %). δ_{H} (300 MHz, CDCl₃), 1.48 (s, 9H), 3.99 (d, 2H, $J = 7.2$ Hz), 5.95 (d, 1H, $J = 15.3$ Hz, $J = 1.2$ Hz), 6.90 ppm (m, 1H)

***(E)*-*tert*-butyl 4-((2-methoxyethyl)amino)but-2-enoate (36)**

(E)-*tert*-butyl 4-bromobut-2-enoate (2.21 g, 10 mmol) was dissolved in 8 ml diethyl ether, potassium carbonate (1.38 g, 10 mmol) was added, followed by addition of 2-methoxyethyl amine (0.30 g, 4 mmol) in a 2 ml of diethyl ether solution via addition funnel. The reaction mixture was stirred overnight at room temperature. After filtration to remove solid, the solution was washed with 10 ml saturated sodium bicarbonate solution, dried, and evaporated. The product was purified via column chromatography, elution gradient from heptane: acetone = 9:1 to 4:1 to give an orange oil product **36** (0.40 g, 47 %). This procedure also obtained orange oil of product **3** (0.50 g, 35 %). *(E)*-*tert*-butyl 4-bromobut-2-enoate was recovered in 36 % yield. δ_{H}

(300 MHz, CDCl₃), 1.47 (s, 9H), 2.79 (t, 2H, $J = 5.1$ Hz), 3.36 (s, 3H), 3.40 (d, 2H, $J = 5.4$ Hz), 3.49 (t, 2H, $J = 5.1$ Hz), 5.90 (dd, 1H, $J = 15.9$ Hz, $J = 1.8$ Hz), 6.90 ppm (m, 1H)

(2*E*,2'*E*)-di-*tert*-butyl 4,4'-((2-methoxyethyl)azanediyl)bis(but-2-enoate) (3)

36 (0.20 g, 0.93 mmol) was dissolved in 1 ml diethyl ether, potassium carbonate (0.12 g, 0.90 mmol) was added, followed by addition of a solution of **35** (0.20 g, 0.90 mmol) in 1 ml of diethyl ether. The reaction was stirred overnight at room temperature. The solid was removed by filtration and the solution was washed with saturated sodium bicarbonate solution (2 ml), dried, and evaporated. The crude product was purified via column chromatography (heptane: acetone = 4:1). Yield 0.18 g (56 %) orange oil product. δ_{H} (300 MHz, CDCl₃), 1.48 (s, 18H), 2.67 (t, 2H, $J = 5.7$ Hz), 3.27 (d, 4H, 4.8 Hz), 3.33 (s, 3H), 3.47 (t, 2H, $J = 5.7$ Hz), 5.90 (d, 2H, $J = 15.6$ Hz), 6.83 ppm (m, 2H)

(3*R*,4*S*,5*S*)-*tert*-butyl 3-(benzyl(*S*)-1-phenylethylamino)-5-(2-(*tert*-butoxy)-2-oxoethyl)-1-(2-methoxyethyl)piperidine-4-carboxylate (39)³⁶

S-(α -methylbenzyl)benzyl amine (0.31 g, 1.4 mmol) was dissolved in 2 ml anhydrous THF under nitrogen. *N*-butyl lithium (1 ml, 1.6 mmol, 1.6M in hexane) was added at -78 °C. The pink solution formed immediately was stirred for 30 min at -78 °C. Compound **3** (0.36 g, 1 mmol), which was dried 24 h by molecular sieve, was dissolved in 3 ml anhydrous THF and the solution was added to the pink solution at -78 °C. The reaction mixture was stirred for 2 h also at -78 °C. The reaction was quenched with 10 % ammonium chloride and warmed to room temperature. 10 ml ethyl acetate was added and the layers were separated. The aqueous phase was further extracted with ethyl acetate (2 x 5 ml). The combined organic phase was washed with saturated

sodium bicarbonate solution (20 ml), dried and evaporated. After purification via column chromatography (heptane: acetone = 4: 1), product was obtained as an orange oil 0.50 g (88 %). δ_{H} (300 MHz, CDCl_3), 1.345 (d, 3H, $J = 6.9$ Hz), 1.40 (s, 9H), 1.47 (s, 9H), 1.51-1.75 (m, 1H), 1.76-2.00 (m, 2H), 2.11 (t, 2H, $J = 11.1$ Hz), 2.16-2.34 (m, 2H), 2.36-2.67 (m, 2H), 2.95 (ddd, 2H, $J = 21$ Hz, $J = 11.1$ Hz, $J = 3.0$ Hz), 3.34 (s, 3H), 3.43 (t, 2H, $J = 5.4$ Hz), 3.76 (quart, 2H, $J = 13.8$ Hz), 4.08 (quart, 1H, $J = 6.6$ Hz), 7.15-7.50 ppm (m, 10H)

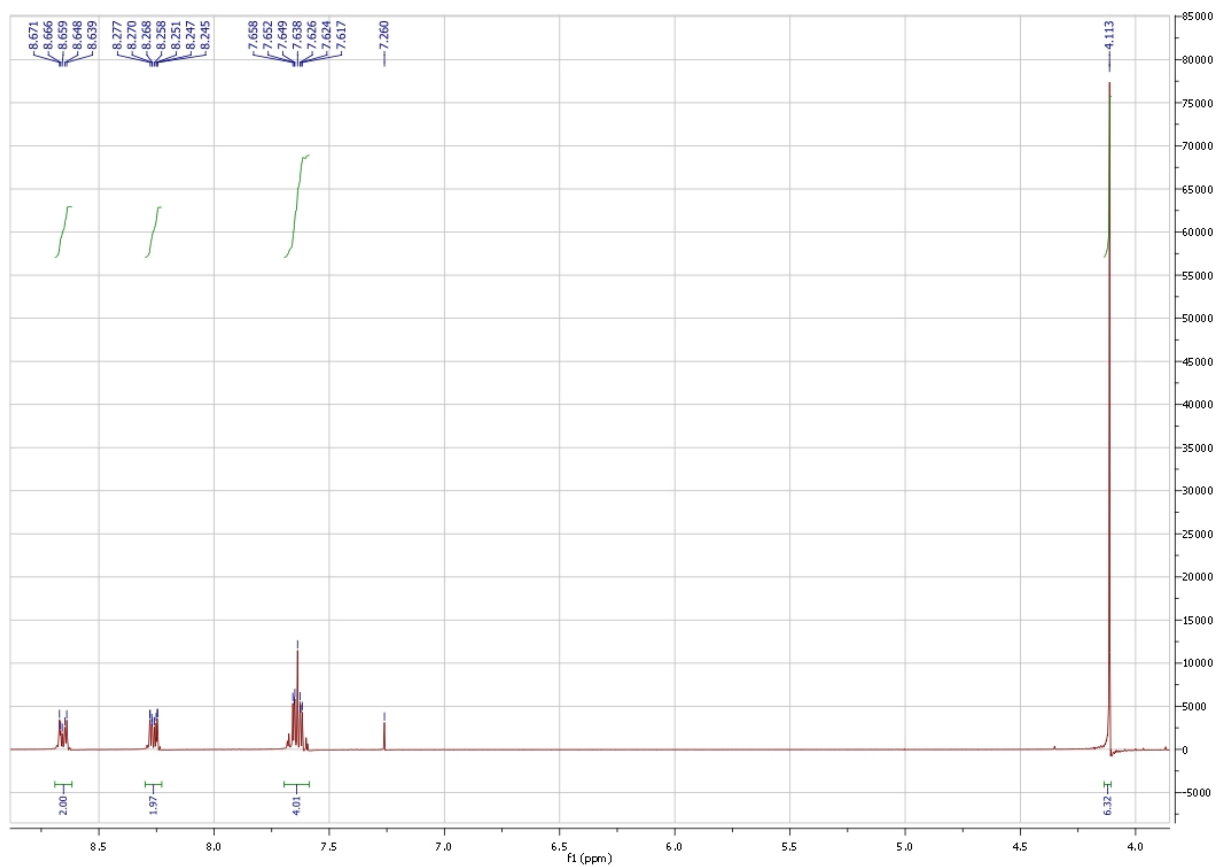
References

1. Karkare, S.; Bhatnagar, D., Promising nucleic acid analogs and mimics: characteristic features and applications of PNA, LNA, and morpholino. *Applied microbiology and biotechnology* **2006**, *71* (5), 575-586.
2. Zamecnik, P. C.; Stephenson, M. L., Inhibition of Rous sarcoma virus replication and cell transformation by a specific oligodeoxynucleotide. *Proceedings of the National Academy of Sciences* **1978**, *75* (1), 280-284.
3. Ray, A.; Nordén, B., Peptide nucleic acid (PNA): its medical and biotechnical applications and promise for the future. *The FASEB Journal* **2000**, *14* (9), 1041-1060.
4. Hyrup, B.; Nielsen, P. E., Peptide nucleic acids (PNA): synthesis, properties and potential applications. *Bioorganic & medicinal chemistry* **1996**, *4* (1), 5-23.
5. Dervan, P. B., Design of sequence-specific DNA-binding molecules. *Science* **1986**, *232* (4749), 464-471.
6. Larsen, H. J.; Bentin, T.; Nielsen, P. E., Antisense properties of peptide nucleic acid. *Biochimica et Biophysica Acta (BBA)-Gene Structure and Expression* **1999**, *1489* (1), 159-166.
7. Nielsen, P. E.; Egholm, M.; Berg, R. H.; Buchardt, O., Sequence-selective recognition of DNA by strand displacement with a thymine-substituted polyamide. *Science* **1991**, *254* (5037), 1497-1500.
8. Stein, C., Phosphorothioate antisense oligodeoxynucleotides: questions of specificity. *Trends in biotechnology* **1996**, *14* (5), 147.
9. Egholm, M.; Buchardt, O.; Christensen, L.; Behrens, C.; Freier, S. M.; Driver, D. A.; Berg, R. H.; Kim, S. K.; Norden, B.; Nielsen, P. E., PNA hybridizes to complementary oligonucleotides obeying the Watson-Crick hydrogen-bonding rules. *Nature* **1993**, *365* (6446), 566-568.
10. Demidov, V. V.; Potaman, V. N.; Frank-Kamenetskii, M.; Egholm, M.; Buchardt, O.; Sönnichsen, S. H.; Nielsen, P. E., Stability of peptide nucleic acids in human serum and cellular extracts. *Biochemical pharmacology* **1994**, *48* (6), 1310-1313.
11. Good, L.; Nielsen, P. E., Inhibition of translation and bacterial growth by peptide nucleic acid targeted to ribosomal RNA. *Proceedings of the National Academy of Sciences* **1998**, *95* (5), 2073-2076.
12. Nielsen, P. E.; Egholm, M.; Buchardt, O., Sequence-specific transcription arrest by peptide nucleic acid bound to the DNA template strand. *Gene* **1994**, *149* (1), 139-145.
13. (a) Hamilton, S. E.; Pitts, A. E.; Katipally, R. R.; Jia, X.; Rutter, J. P.; Davies, B. A.; Shay, J. W.; Wright, W. E.; Corey, D. R., Identification of determinants for inhibitor binding within the RNA active site of human telomerase using PNA scanning. *Biochemistry* **1997**, *36* (39), 11873-11880; (b) Norton, J. C.; Piatyszek, M. A.; Wright, W. E.; Shay, J. W.; Corey, D. R., Inhibition of human telomerase activity by peptide nucleic acids. *Nature biotechnology* **1996**, *14* (5), 615-619.
14. Ørum, H.; Nielsen, P. E.; Egholm, M.; Berg, R. H.; Buchardt, O.; Stanley, C., Single base pair mutation analysis by PNA directed PCR clamping. *Nucleic Acids Research* **1993**, *21* (23), 5332-5336.
15. Veselkov, A. G.; Demidov, V. V.; Nielsen, P. E.; Frank-Kamenetskii, M. D., A new class of genome rare cutters. *Nucleic acids research* **1996**, *24* (13), 2483-2487.
16. Singh, S. K.; Koshkin, A. A.; Wengel, J.; Nielsen, P., LNA (locked nucleic acids): synthesis and high-affinity nucleic acid recognition. *Chemical communications* **1998**, (4), 455-456.
17. Braasch, D. A.; Corey, D. R., Locked nucleic acid (LNA): fine-tuning the recognition of DNA and RNA. *Chem. Biol* **2001**, *8* (1), 7.
18. Gotfredsen, C. H.; Schultze, P.; Feigon, J., Solution structure of an intramolecular pyrimidine-purine-pyrimidine triplex containing an RNA third strand. *Journal of the American Chemical Society* **1998**, *120* (18), 4281-4289.
19. CROOKE, S. T., Molecular mechanisms of antisense drugs: RNase H. *Antisense and Nucleic Acid Drug Development* **1998**, *8* (2), 133-134.

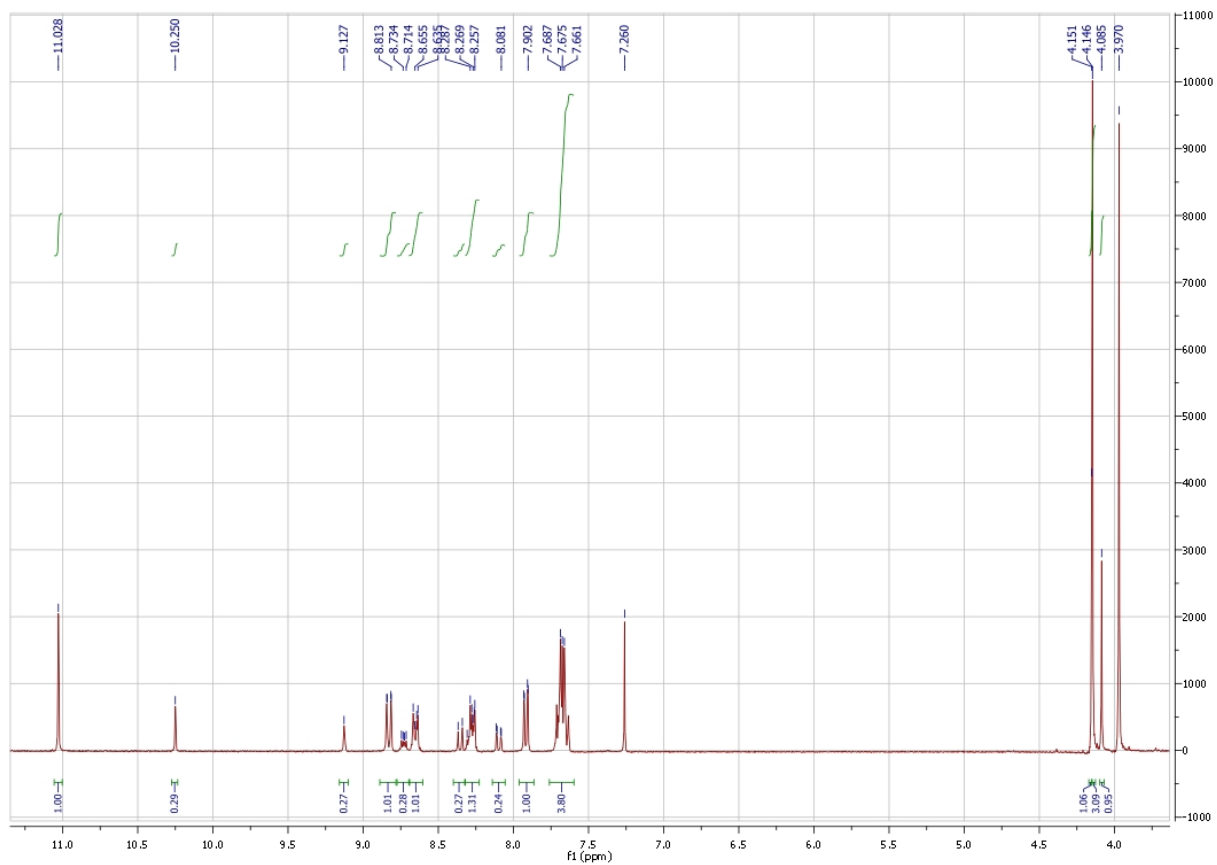
20. Wahlestedt, C.; Salmi, P.; Good, L.; Kela, J.; Johnsson, T.; Hökfelt, T.; Broberger, C.; Porreca, F.; Lai, J.; Ren, K., Potent and nontoxic antisense oligonucleotides containing locked nucleic acids. *Proceedings of the National Academy of Sciences* **2000**, *97* (10), 5633-5638.
21. Jakobsen, M. R.; Haasnoot, J.; Wengel, J.; Berkhout, B.; Kijms, J., Efficient inhibition of HIV-1 expression by LNA modified antisense oligonucleotides and DNAszymes targeted to functionally selected binding sites. *Retrovirology* **2007**, *4* (1), 29.
22. Elayadi, A. N.; Braasch, D. A.; Corey, D. R., Implications of high-affinity hybridization by locked nucleic acid oligomers for inhibition of human telomerase. *Biochemistry* **2002**, *41* (31), 9973-9981.
23. Vester, B.; Lundberg, L. B.; Sørensen, M. D.; Babu, B. R.; Douthwaite, S.; Wengel, J., LNAszymes: incorporation of LNA-type monomers into DNAszymes markedly increases RNA cleavage. *Journal of the American Chemical Society* **2002**, *124* (46), 13682-13683.
24. Simeonov, A.; Nikiforov, T. T., Single nucleotide polymorphism genotyping using short, fluorescently labeled locked nucleic acid (LNA) probes and fluorescence polarization detection. *Nucleic acids research* **2002**, *30* (17), e91-e91.
25. Ørum, H.; Jakobsen, M. H.; Koch, T.; Vuust, J.; Borre, M. B., Detection of the factor V Leiden mutation by direct allele-specific hybridization of PCR amplicons to photoimmobilized locked nucleic acids. *Clinical chemistry* **1999**, *45* (11), 1898-1905.
26. Summerton, J., Uncharged nucleic acid analogs for therapeutic and diagnostic applications: Oligomers assembled from ribose-derived subunits. *Advances in Applied Biotechnology Series* **1989**, *2*, 71-80.
27. SUMMERTON, J.; WELLER, D., Morpholino antisense oligomers: design, preparation, and properties. *Antisense and Nucleic Acid Drug Development* **1997**, *7* (3), 187-195.
28. (a) Nasevicius, A.; Ekker, S. C., Effective targeted gene 'knockdown' in zebrafish. *Nature genetics* **2000**, *26* (2), 216-220; (b) Ekker, S. C., Morphants: a new systematic vertebrate functional genomics approach. *Yeast* **2000**, *17* (4), 302-306.
29. Heasman, J.; Kofron, M.; Wylie, C., β Catenin Signaling Activity Dissected in the Early Xenopus Embryo: A Novel Antisense Approach. *Developmental biology* **2000**, *222* (1), 124-134.
30. Zhang, L.; Peritz, A.; Meggers, E., A simple glycol nucleic acid. *Journal of the American Chemical Society* **2005**, *127* (12), 4174-4175.
31. Herdewijn, P., TNA as a potential alternative to natural nucleic acids. *Angewandte Chemie International Edition* **2001**, *40* (12), 2249-2251.
32. Langkjær, N.; Pasternak, A.; Wengel, J., UNA (unlocked nucleic acid): a flexible RNA mimic that allows engineering of nucleic acid duplex stability. *Bioorganic & medicinal chemistry* **2009**, *17* (15), 5420-5425.
33. Lauri, G.; Bartlett, P. A., CAVEAT: a program to facilitate the design of organic molecules. *Journal of computer-aided molecular design* **1994**, *8* (1), 51-66.
34. Davies, S. G.; Ichihara, O., Asymmetric synthesis of R- β -amino butanoic acid and S- β -tyrosine: Homochiral lithium amide equivalents for Michael additions to α , β -unsaturated esters. *Tetrahedron: Asymmetry* **1991**, *2* (3), 183-186.
35. Urones, J. G.; Garrido, N. M.; Díez, D.; Dominguez, S. H.; Davies, S. G., Conjugate addition to (α , β)(α' , β')-diendioate esters by lithium (α -methylbenzyl) benzylamide: tandem addition-cyclisation versus double addition. *Tetrahedron: Asymmetry* **1999**, *10* (9), 1637-1641.
36. Davies, S. G.; Díez, D.; Dominguez, S. H.; Garrido, N. M.; Kruchinin, D.; Price, P. D.; Smith, A. D., Cyclic β -amino acid derivatives: synthesis via lithium amide promoted tandem asymmetric conjugate addition-cyclisation reactions. *Organic & biomolecular chemistry* **2005**, *3* (7), 1284-1301.
37. Ozeki, M.; Ochi, S.; Hayama, N.; Hosoi, S.; Kajimoto, T.; Node, M., One-Pot Construction of Multiple Contiguous Chiral Centers Using Michael Addition of Chiral Amine. *The Journal of Organic Chemistry* **2010**, *75* (12), 4201-4211.
38. PARUCH, K.; VYKLYCKY, L.; KATZ, T. J., Preparation of 9, 10-dimethoxyphenanthrene and 3, 6-diacetyl-9, 10-dimethoxyphenanthrene. *Organic syntheses* **2003**, *80*, 227-232.

39. Rieche, A.; Gross, H.; Höft, E., Über α -Halogenäther, IV. Synthesen aromatischer Aldehyde mit Dichlormethyl-alkyläthern. *Chemische Berichte* **1960**, *93* (1), 88-94.
40. Speck, M.; Niethammer, D.; Senge, M. O., Isomeric porphyrin phenanthrenequinones: synthesis, NMR spectroscopy, electrochemical properties, and in situ EPR/ENDOR studies of the o-semiquinone anion radicals. *Journal of the Chemical Society, Perkin Transactions 2* **2002**, (3), 455-462.
41. Schlosser, M.; Bailly, F., Embedding an allylmetal dimer in a chiral cavity: The unprecedented stereoselectivity of a twofold Wittig [1, 2]-Rearrangement. *Journal of the American Chemical Society* **2006**, *128* (50), 16042-16043.
42. Chawla, H. M.; Mittal, R. S., Oxidative nitration by silica gel-supported cerium (IV) ammonium nitrate. *Synthesis* **2002**, *1985* (01), 70-72.
43. Yazdanbakhsh, M.; Giasi, M.; Mohammadi, A., Synthesis and solvatochromic properties of some new disperse azo dyes derived from 2-anilinoethanol. *Journal of Molecular Liquids* **2009**, *144* (3), 145-148.
44. Schoutissen, H., The Diazotization of Very Weakly Basic Amines. *Journal of the American Chemical Society* **1933**, *55* (11), 4531-4534.
45. Frøyen, P.; Juvvik, P., HYDRAZONES FROM YLIDES AND DIAZONIUM SALTS: A CONVENIENT SPOT TEST FOR STABILIZED YLIDES OF PHOSPHORUS, ARSENIC, AND SULFUR. *Phosphorus, Sulfur, and Silicon and the Related Elements* **1992**, *69* (1-2), 83-91.
46. Marinescu, L.; Thinggaard, J.; Thomsen, I. B.; Bols, M., Radical azidonation of aldehydes. *The Journal of Organic Chemistry* **2003**, *68* (24), 9453-9455.
47. Orsini, F.; Pelizzoni, F.; Ricca, G., Zinc (0)-mediated formation of carbon-carbon bond from γ -bromo crotonate. *Synthetic Communications* **1982**, *12* (14), 1147-1154.
48. Jung, S. H.; Hwang, G.-S.; Lee, S. I.; Ryu, D. H., Total Synthesis of (+)-Ambuic Acid: α -Bromination with 1, 2-Dibromotetrachloroethane. *The Journal of Organic Chemistry* **2012**, *77* (5), 2513-2518.

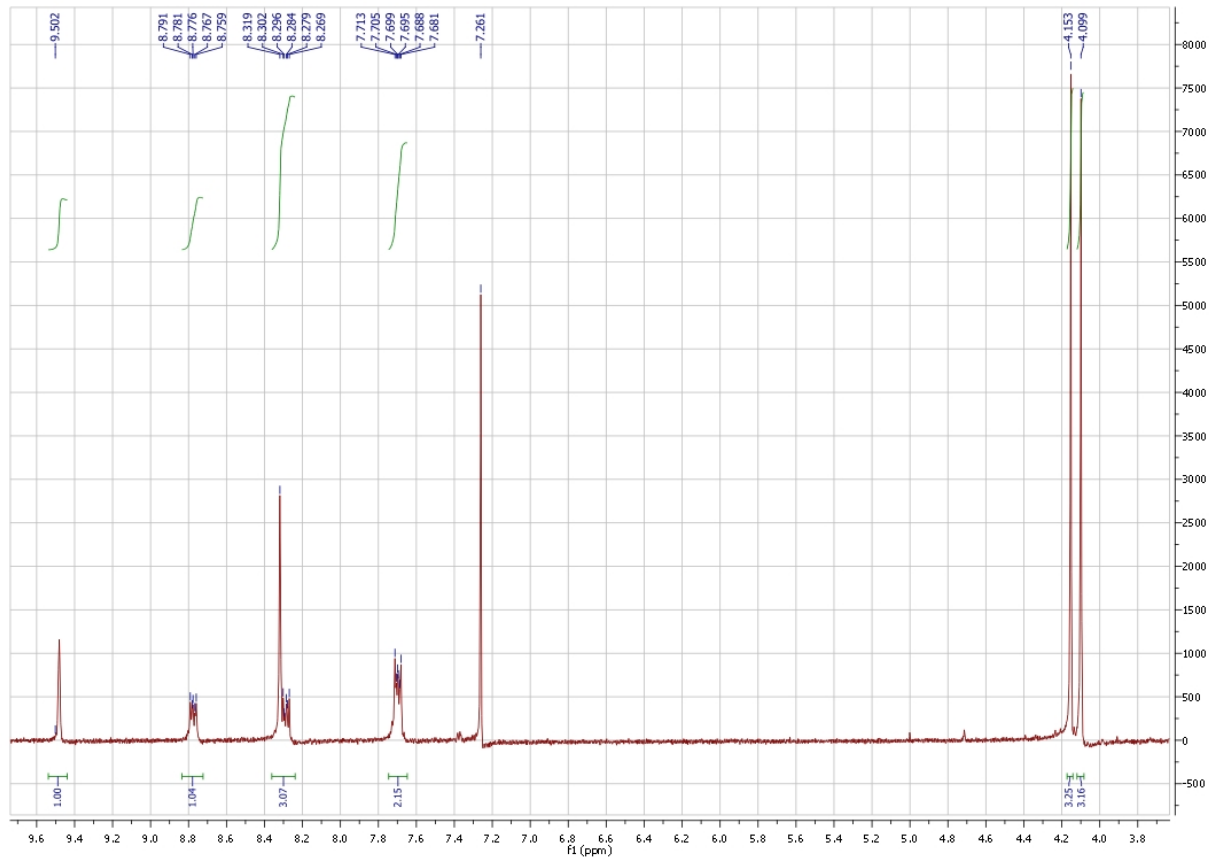
Appendix



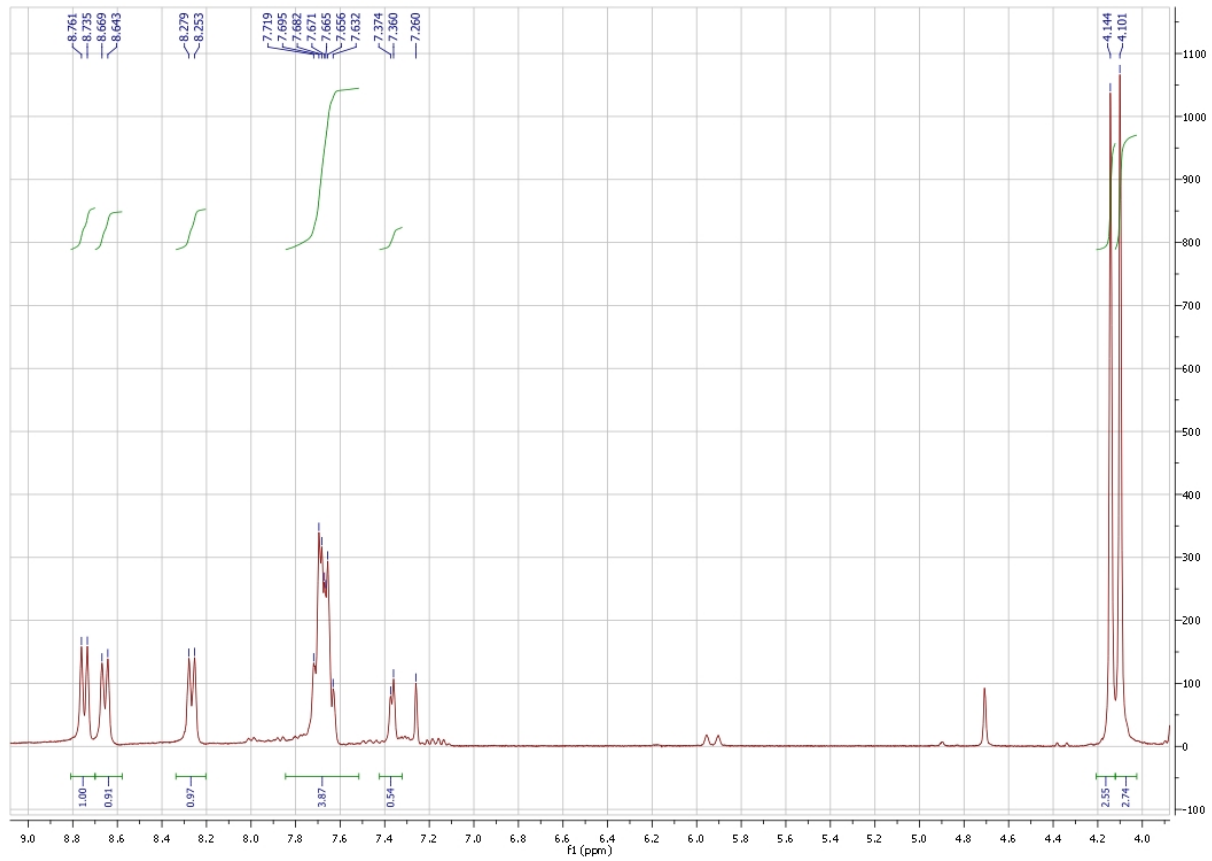
9,10-dimethoxyphenanthrene (18)



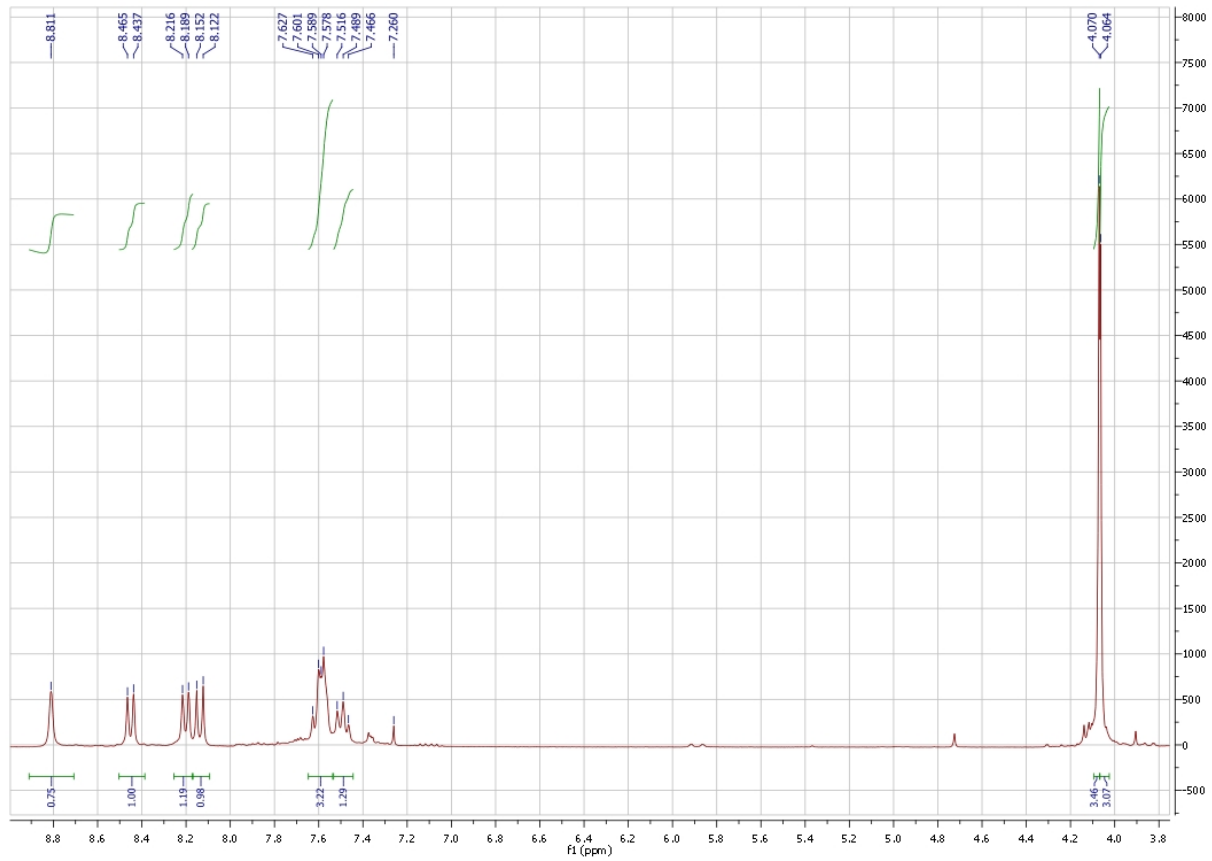
Mixture of 9,10-dimethoxyphenanthrene-3-carbaldehyde (19) and 9,10-dimethoxyphenanthrene-1-carbaldehyde (20)



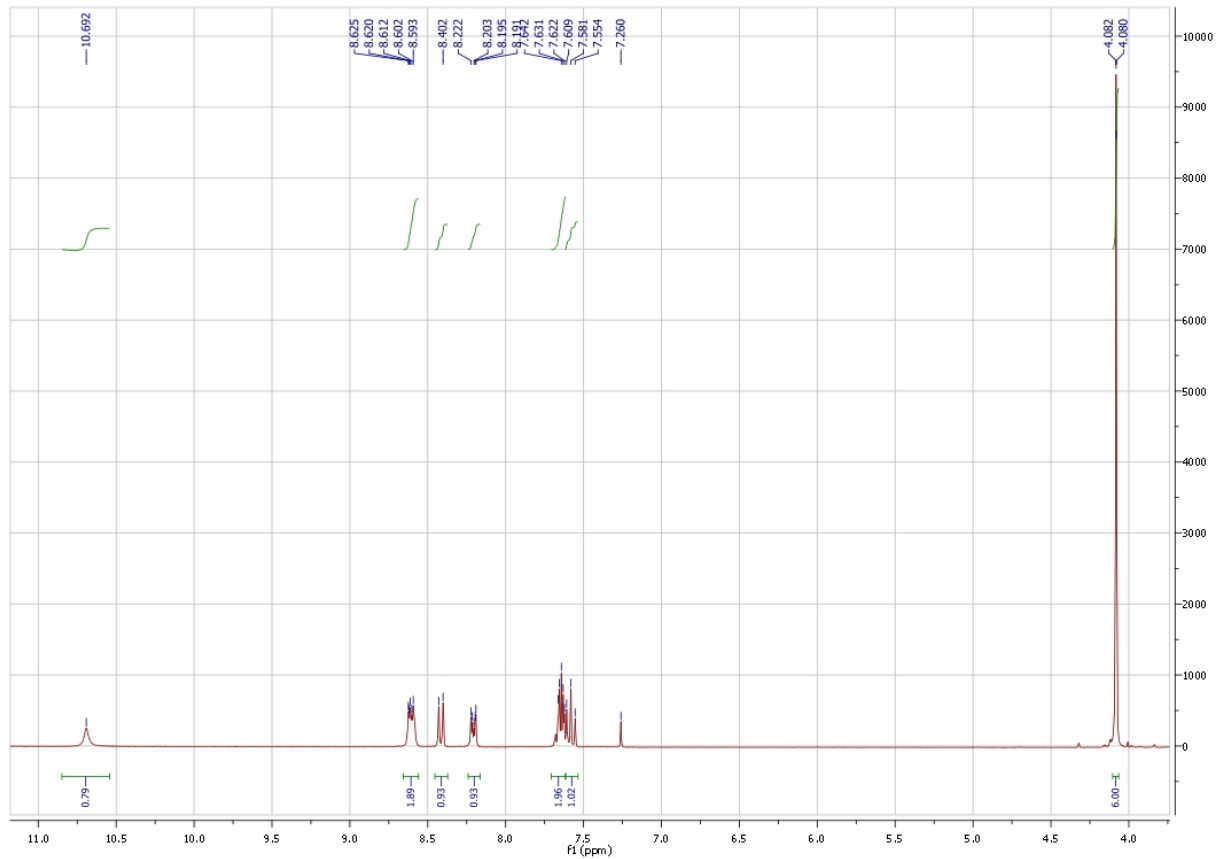
9,10-dimethoxyphenanthrene-3-carboxylic acid (15)



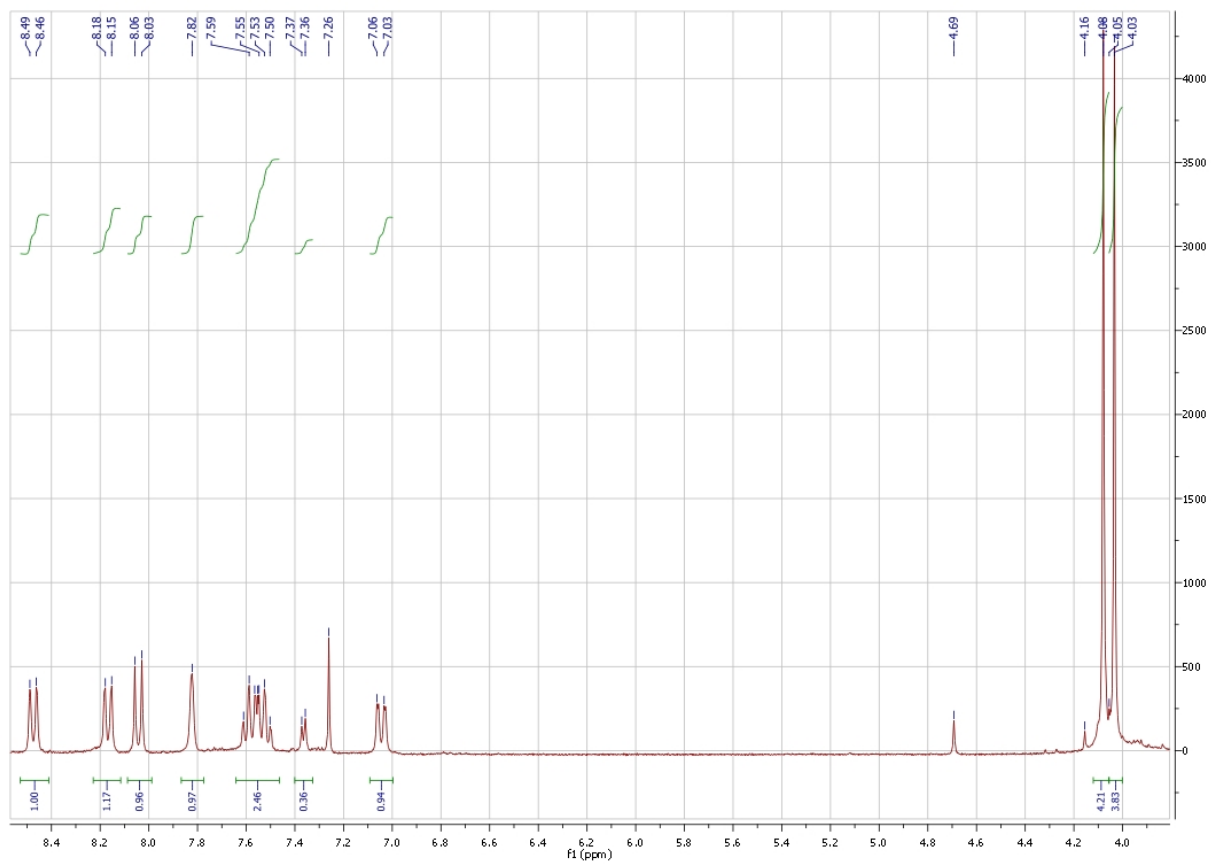
9,10-dimethoxyphenanthrene-1-carboxylic acid (21)



(9,10-dimethoxyphenanthren-3-yl)carbamoyl azide (30)



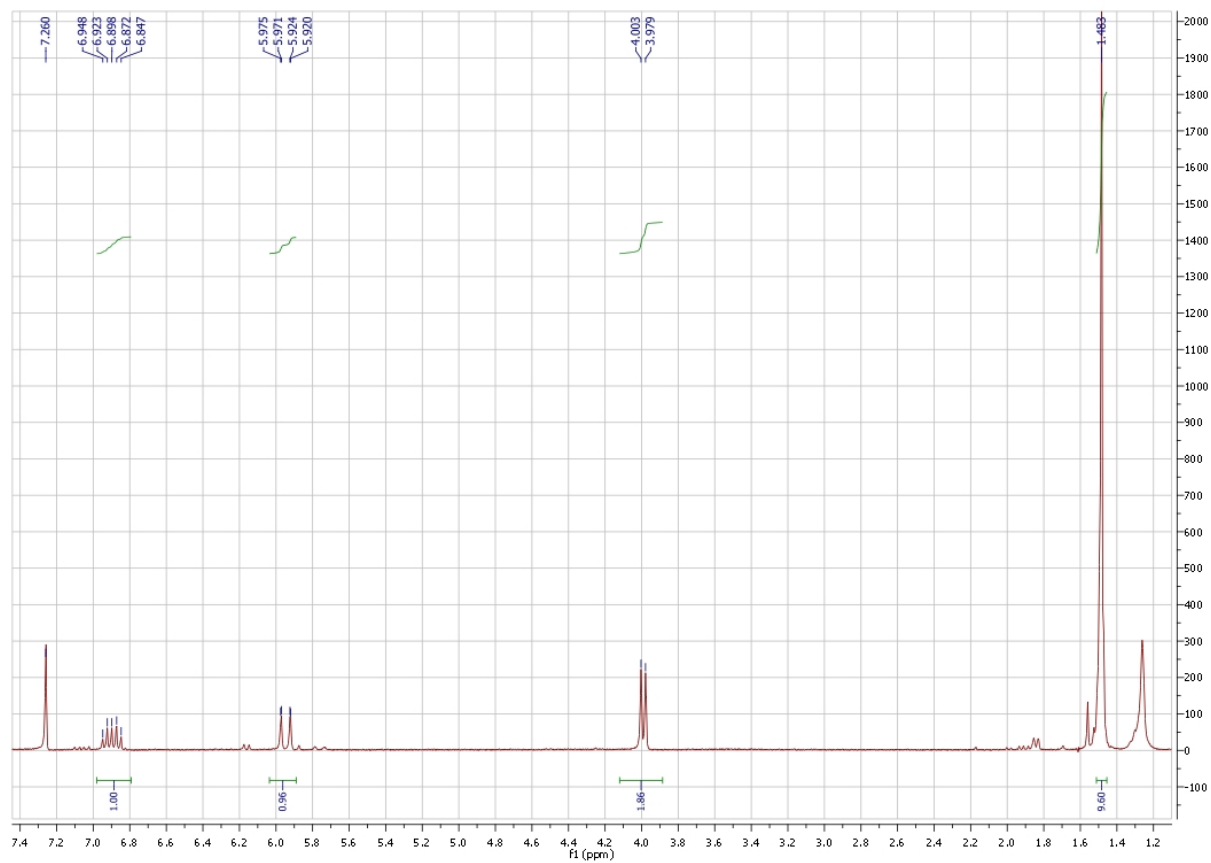
(9,10-dimethoxyphenanthren-1-yl)carbamoyl azide (31)



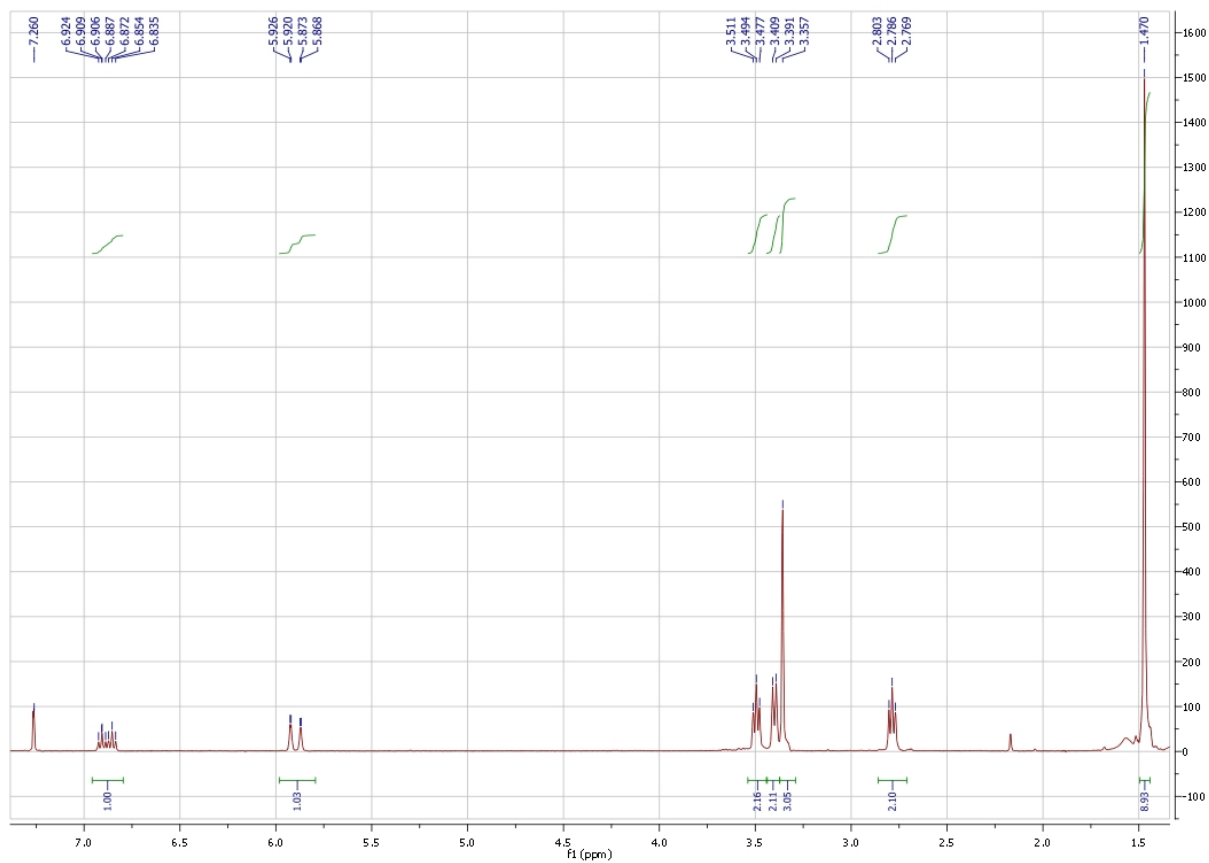
9,10-dimethoxyphenanthrene-3-amine (14)



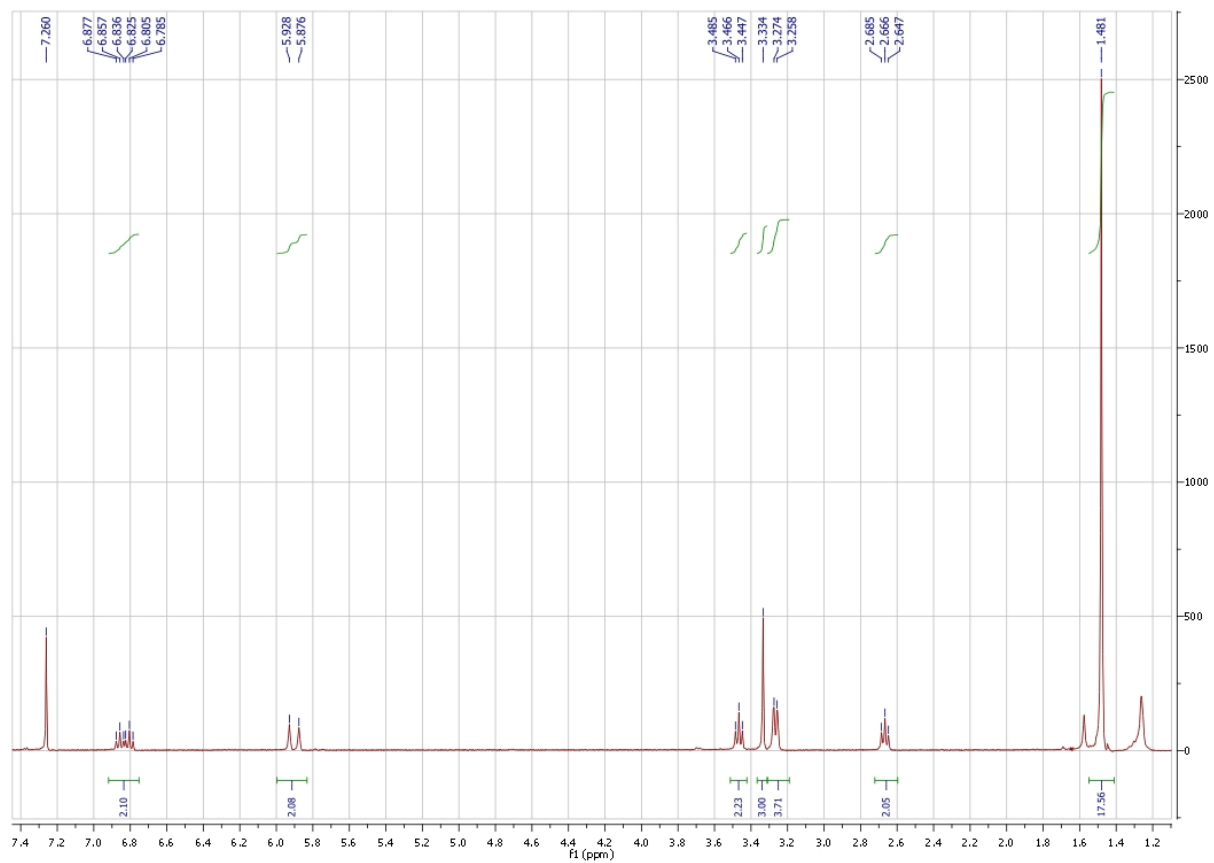
tert-butyl crotonate (34)



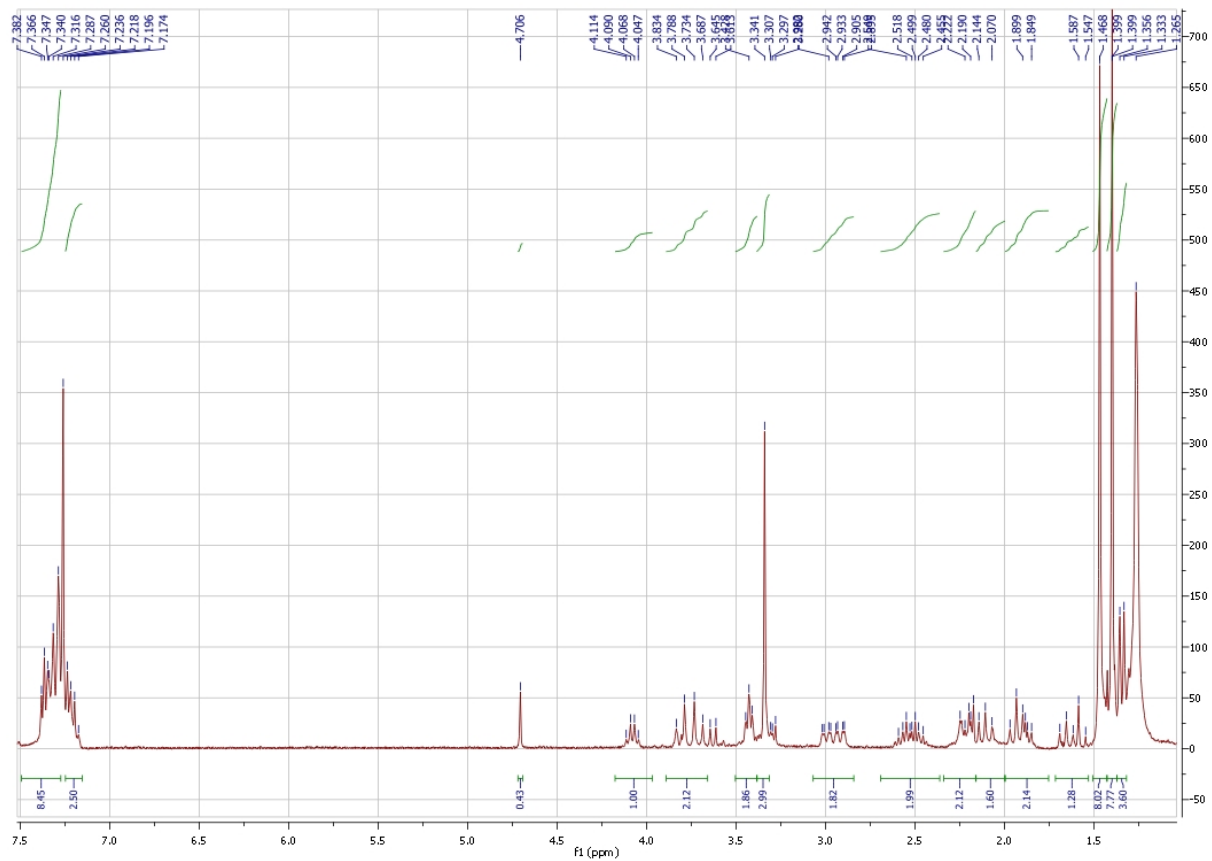
t-butyl- γ -bromo crotonate (35)



(*E*)-*tert*-butyl 4-((2-methoxyethyl)amino)but-2-enoate (36)



(2*E*,2'*E*)-di-*tert*-butyl 4,4'-((2-methoxyethyl)azanediyl)bis(but-2-enoate) (3)



(3*R*,4*S*,5*S*)-*tert*-butyl 3-(benzyl(*S*)-1-phenylethyl)amino)-5-(2-(*tert*-butoxy)-2-oxoethyl)-1-(2-methoxyethyl)piperidine-4-carboxylate (39)